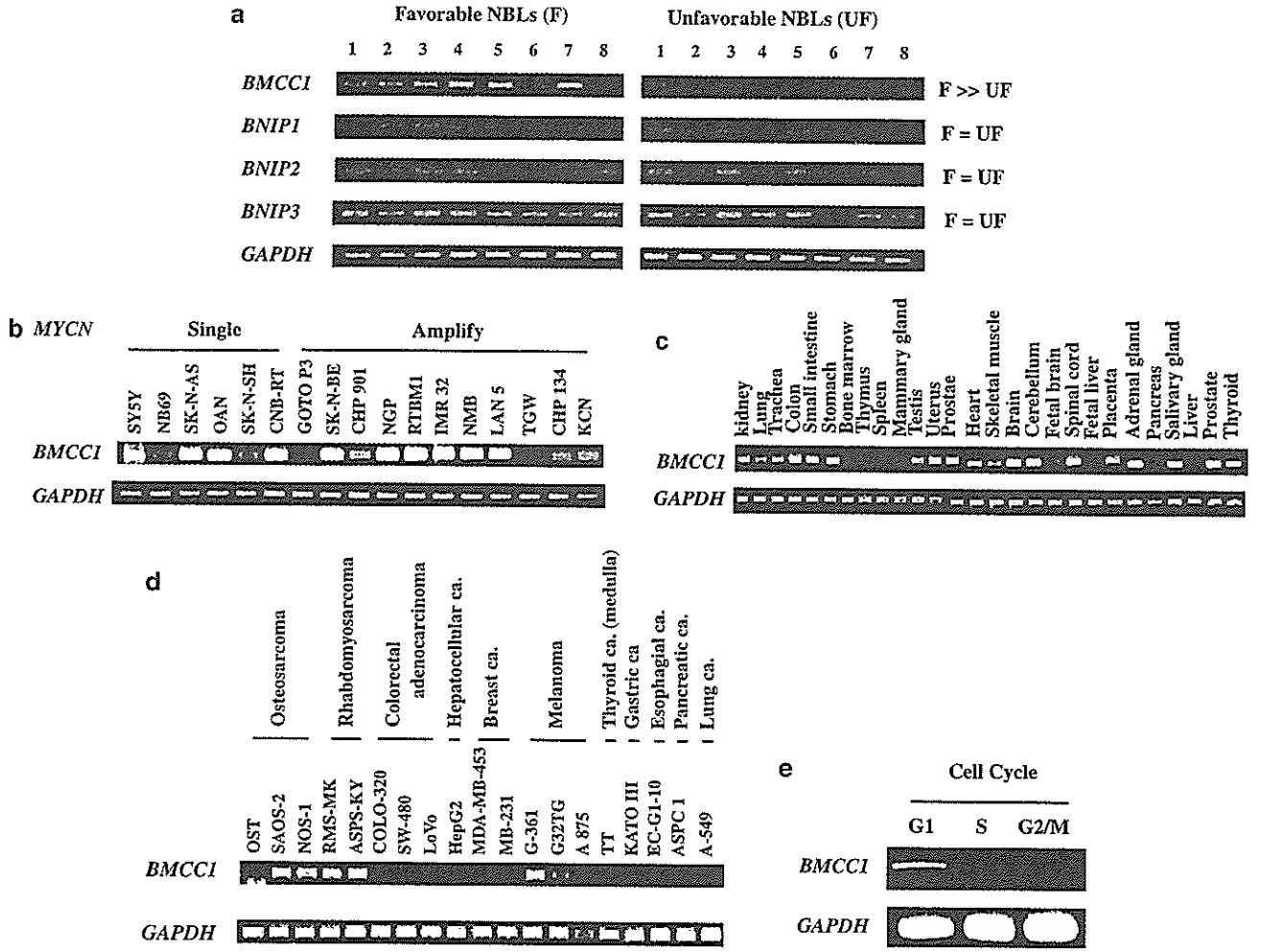

Figure 2 Expression of *BMCC1* mRNA. (**a**) Differential expression of *BMCC1* in favorable and unfavorable neuroblastomas. mRNA expression patterns for *BMCC1* and *BNIP* gene family members were detected by semiquantitative RT–PCR procedure. Results for eight favorable and eight unfavorable NBLs are shown. The expression of *GAPDH* is also shown as a control. Lanes 1–8: favorable NBLs (F; stage 1 or 2, with a single copy of *MYCN*), lanes 9–6: unfavorable NBLs (UF; stage 3 or 4, with *MYCN* amplification). (**b**) Expression of *BMCC1* mRNA in neuroblastoma cell lines. In all, 11 NBL cell lines with *MYCN* amplification and six cell lines with a single copy of *MYCN* were used for semiquantitative RT–PCR as templates. (**c**) Semiquantitative RT–PCR of *BMCC1* in multiple human tissues. Total RNA of 25 adult tissues and two fetal tissues were purchased from Clontech Co. Ltd. As a control, same cDNA templates were amplified by *GAPDH* primers. (**d**) Expression of *BMCC1* mRNA in the other cancer cell lines. Semiquantitative RT–PCR analysis was performed using cDNA primers and control *GAPDH* primers. Tumor origins were shown on the top. (**e**) The changes in expression of *BMCC1* at the cell cycle stages. HeLa cells were synchronized by treatment with 400 μM mimosine for 18 h (G1-phase arrest), with 2 mM thymidine for 20 h (S-phase arrest), or with 0.6 μg/ml nocodazole for 18 h (G2/M-phase arrest) and collected for RNA isolation. Semiquantitative RT–PCR was conducted by using *BMCC1* primers and *GAPDH* control primers.

coma, melanoma and some osteosarcoma cell lines, whereas only low levels of expression were found in cancer cell lines of liver, breast, thyroid and colon (Figure 2d). We further examined the cell cycle-dependent expression of *BMCC1* mRNA in HeLa cells by using semiquantitative RT–PCR. As shown in Figure 2e, *BMCC1* was predominantly expressed in G1 phase of the cell cycle.

In situ *hybridization of* BMCC1 *in mouse embryo*

In situ hybridization in mouse embryo showed that *BMCC1* was specifically expressed in neural tube and neural crest-related tissues. In E10.5 mouse embryo, *BMCC1* was highly expressed in neural tube and pharyngeal arches which are derived from neural crest. The expression of *BMCC1* seemed to be more restricted in the later stages of development (Figure 3). In E12.5 mouse embryo (Figure 3d), *BMCC1* was expressed in spinal cord, hindbrain, midbrain, forebrain and dorsal root ganglia (DRG). Although the expressions of *BMCC1* in E14.5 mouse embryos (Figure 3a and b) were similar to those in E12.5, the regions expressing *BMCC1* in hindbrain (Figure 3a), spinal cord and forebrain at E14.5 (Figure 3b) were more dorsally restricted than at E12.5.

Immunohistochemical staining of BMCC1 in primary NBLs

The favorable NBLs occasionally expressed BMCC1 in the cytoplasm of the tumor cells (Figure 4b). In contrast,

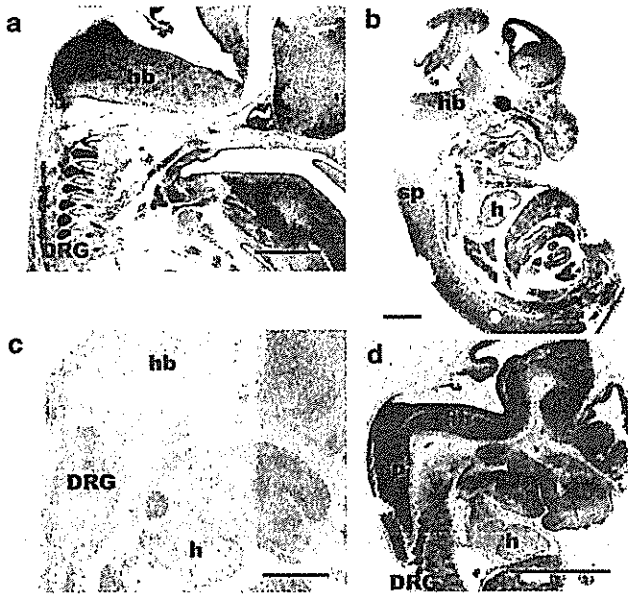

Figure 3 Section *in situ* hybridization of embryos with the *BMCC1* probe. Sagittal sections of embryos at E14.5 (a–c) and E12.5 (d) were prepared and the *BMCC1* expression was examined by section *in situ* hybridization. (a), (b) and (d) Antisense probes. (c) Sense probe (control). The *BMCC1* probe used is described in the Experimental procedures. DRG, dorsal root ganglion; sp, spinal cord; hb, hindbrain; h, heart. Scale bar, 200 μm.

in the unfavorable neuroblastomas the tumor cells were entirely negative for BMCC1 or only a few positive cells were observed (Figure 4d).

Prognostic significance of BMCC1 *mRNA expression in human NBLs*

The levels of *BMCC1* mRNA expression were measured in 98 primary NBLs by using quantitative real-time RT–PCR. The high levels of *BMCC1* expression were significantly associated with favorable NBL in stages 1, 2 and 4 (Figure 4e). The high levels of *BMCC1* expression was significantly associated with young age ($P<0.00005$), favorable stages ($P<0.00005$), high expression of *TrkA* mRNA ($P<0.00005$), single copy of *MYCN* ($P<0.00005$), tumors found by mass screening (MS) ($P<0.00005$), nonadrenal origin ($P=0.0025$) according to the Student's *t*-test. The log-rank test showed that the high expression of *BMCC1* was significantly correlated with a favorable outcome ($P=0.0008$) as shown in the Kaplan–Meier cumulative survival curves (Table 1 and Figure 4f).

The multivariate Cox regression analysis also demonstrated that *BMCC1* expression (high vs low), age (<1 year vs ⩾1 year), *MYCN* copy number (1 copy vs >1 copy), and MS (positive tumors vs sporadic tumors) had prognostic significance ($P<0.0005$) (Table 2). *BMCC1* expression was significantly related to survival ($P=0.007$) after controlling age ($P=0.018$). However, it lost significance in a model including jointly with *MYCN* amplification or MS. Furthermore, *BMCC1* expression was significantly related to survival ($P=0.027$) after controlling age ($P=0.014$) and origin ($P=0.403$).

Changes in BMCC1 *mRNA expression during neuronal differentiation and apoptosis*

To examine whether exogenous expression of BMCC1 affects the cell growth of neuronal PC12 cells, a rat pheochromocytoma cell line, we transfected the cells with a full-length *BMCC1* cDNA. The overexpression of BMCC1 appeared to decrease the cell growth but the result was not statistically significant (data not shown). We then tested if expression of *BMCC1* mRNA was changed during neuronal differentiation and/or apoptosis. For that purpose, we used three different neuronal cell lines. The NT2 cell line, which was established from human immature teratocarcinoma and the cells show astrocytic differentiation after treatment with retinoic acid (RA) (Moasser *et al*., 1996). The CHP134 NBL cells undergo apoptosis after 3 days of the treatment with RA (Islam *et al*., 2000). On the other hand, the RTBM1 human NBL cells are induced to differentiate after the treatment with RA (Nakamura *et al*., 1998). We have confirmed that caspase 3 expression was increased in CHP134 cells but decreased in RTBM1 cells at day 7 after treatment with RA by semiquantitative RT–PCR. On the other hand, nestin expression was not changed in the former and slightly increased in the latter (Figure 5a). Expression of *BMCC1* mRNA was downregulated during RA-induced neuronal differentiation in both NT2 and RTBM1 cells, whereas it was rather upregulated in CHP134 cells on day 7 after the treatment with RA when many cells were undergoing apoptosis (Figure 5a).

To further confirm the above observation seen in neuronal cell lines, we examined the changes in *BMCC1* expression in superior cervical ganglion (SCG) neurons obtained from newborn mice in primary culture. The cultured cells were treated with 50 ng/ml NGF for 5 days (induction of neuronal differentiation) and then depleted NGF from the medium and added anti-NGF antibodies to induce neuronal apoptosis. As shown in Figure 5b, induction of differentiation by NGF decreased expression of *BMCC1*, whereas the NGF-depletion-induced apoptosis was accompanied with increase in *BMCC1* expression. This was very similar to the changes in expression of *c-jun* and *Bim* which had already been reported (Whitfield *et al*., 2001). Thus, the levels of *BMCC1* mRNA are changed during neuronal differentiation and apoptosis in an opposite manner.

Enhanced NGF-depletion-induced apoptosis in SCG neurons obtained from BMCC1 transgenic mice

We next generated *BMCC1* transgenic mice by using the expression construct with the tyrosine hydroxylase promoter-driven promoter to examine the functional role of BMCC1 in the sympathetic neurons. The SCG neurons obtained from either control or transgenic newborn mice were subjected to primary culture. The integration of the BMCC1 in the mouse genome and its overexpression in SCG neurons were confirmed by both

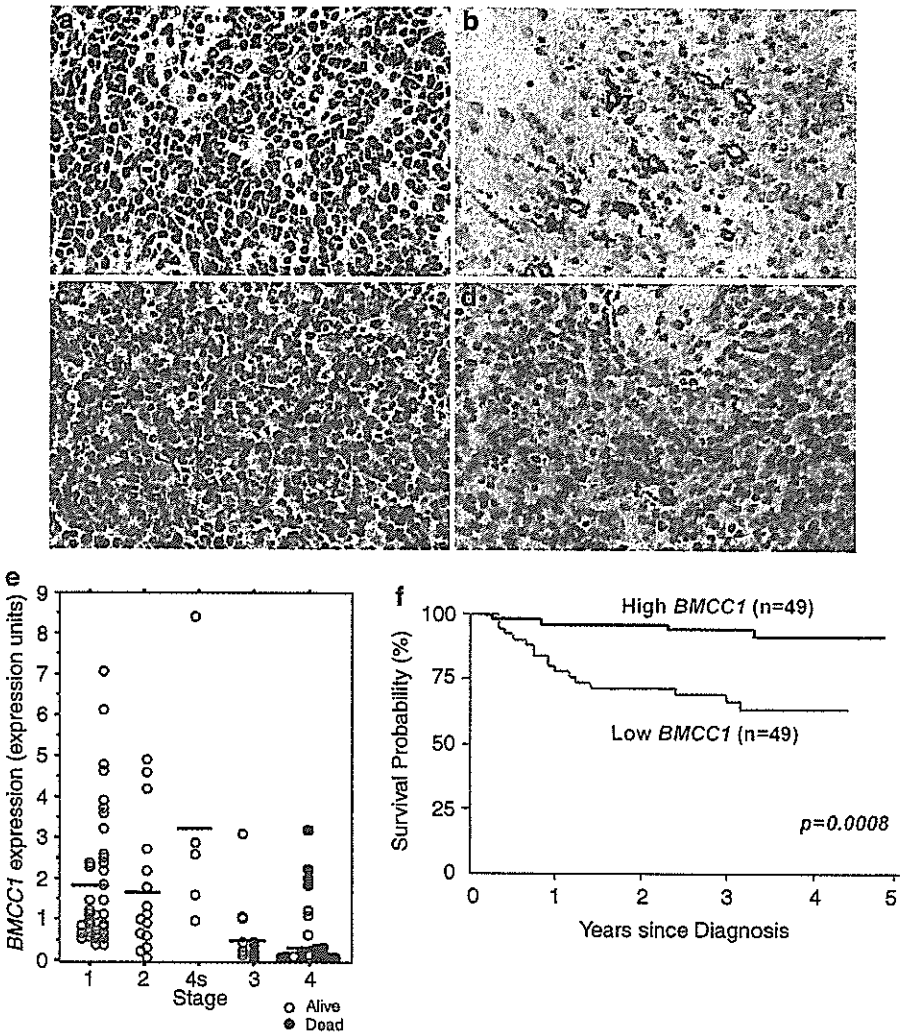

Figure 4 Immunohistochemistry and prognostic significance of BMCC1 expression in primary neuroblastomas. (**a**) and (**b**) In the favorable neuroblastoma without *MYCN* amplification, the tumor cells are occasionally positive for BMCC1 in the cytoplasm. (**c**) and (**d**) The unfavorable neuroblastoma with *MYCN* amplification is negative for BMCC1. (**a**) and (**c**) Hematoxylin–eosin staining. (**b**) and (**d**) BMCC1 immunostaining. (**e**) Low expression of *BMCC1* is associated with poor prognosis of the patients with neuroblastoma. Real-time quantitative RT–PCR analysis of *BMCC1* in 98 tumor samples from patients with neuroblastomas according to tumor stage. The levels of expression of *BMCC1* were normalized to that of *GAPDH*. Horizontal lines; group means, open circles; patients alive, solid circles, patients deceased. (**f**) Cumulative survival curves of patients with neuroblastoma, according to expression of *BMCC1* mRNA. The Kaplan–Meier curves show the probability of survival in terms of the level of expression of *BMCC1*. The survival curves were analysed by the Mantel–Haenszel log-rank test.

RT–PCR (Figure 6a) and Western blot (data not shown). The treatment of the transgenic SCG neurons with NGF in primary culture induced neurite extension similarly to control cells, but induction of apoptosis after depleting NGF was significantly enhanced in the cells overexpressing BMCC1 (Figure 6b–d). This suggested that BMCC1 overexpression may function as proapoptotic in neuronal cells.

Discussion

The presence of the highly conserved BCH domain in BMCC1 suggests its role in the regulation of apoptosis. BNIP2, which shares the BCH domain with BMCC1, has originally been identified as a molecule interacting with the adenovirus E1B 19-kDa protein. The E1B protein protects the cells from apoptosis induced by viral infection or other proapoptotic stimuli (Gooding *et al*., 1991; Hashimoto *et al*., 1991; White *et al*., 1992; Boyd *et al*., 1994). Bcl-2 and its related antiapoptotic proteins can functionally substitute for the E1B 19-kDa protein and bind to BNIP2. Therefore, it has been suggested that BNIP2 is a potential proapoptotic protein (Subramanian *et al*., 1995).

On the other hand, Cdc42 regulates the activation of the c-Jun amino-terminal kinase (JNK) in various cells (Bagrodia *et al*., 1995; Coso *et al*., 1995; Zhang *et al*., 1995). Cdc42 induces an apoptosis mediated by the JNK–MAP kinase cascade in Jurkat T lymphocytes (Chuang *et al*., 1997). The apoptosis is prevented by inhibitors of caspases, suggesting that activation of the

Table 1 Prognostic significance of *BMCC1* expression, age, stage, *TrkA* expression, *MYCN* amplification, mass screening and tumor origin in primary neuroblastomas (log-rank tests)

Variable	*t-tests*			*Log-rank tests*		
	Number of patients	*Mean±s.e.m. (BMCC1 exp.)*	P-*value*	*Number of deaths*	*Number of expected deaths*	P-*value*
BMCC1 expression						0.0008
Low	49			17	9.39	
High	49			4	11.61	
Age (year)						<0.00005
<1	63	1.82±0.23	<0.00005	5	14.55	
⩾1	35	0.64±0.15		16	6.45	
Tumor stage						<0.00005
1, 2, 4s	59	1.97±0.23	<0.00005	0	14.57	
3, 4	39	0.55±0.13		21	6.43	
TrkA *expression*						<0.00005
Low	44	0.91±0.22	<0.00005	21	7.75	
High	54	1.81±0.25		0	13.25	
MYCN *copy number*[a]						<0.00005
Amplified	27	0.30±0.10	<0.00005	18	4.14	
Single	70	1.80±0.20		3	16.86	
Mass screening						<0.00005
Positive	55	1.87±0.22	<0.0025	1	13.32	
Negative	43	0.80±0.22		20	7.68	
Origin						0.061
Adrenal gland	62	1.11±0.20	<0.00005	17	12.82	
Others	36	1.91±0.25		4	8.18	

[a]One patient who had missing *MYCN* information was excluded from analysis.

JNK pathway by Cdc42 is regulated by caspases. The interactive regulation between activation of JNK pathway and that of caspase cascade has also been reported in other biological systems (Cahill *et al*., 1996; Juo *et al*., 1997; Lenczowski *et al*., 1997; Seimiya *et al*., 1997). Cdc42 is also known to function as an initiator of neuronal cell death by activating a c-Jun-regulated transcriptional machinery (Bazenet *et al*., 1998). Cdc42GAP is a Cdc42-activating protein and, like Cdc42, binds to BNIP2 through the BCH domain when it is dephosphorylated at the tyrosine residue. Thus, the proteins with the BCH domain including BMCC1 seem to function in the regulation of apoptosis. The 'EYV' motif in the BCH domain, which is necessary for binding BNIP2 and Cdc42, is also conserved in the same domain of BMCC1. The role of P-loop in the regulation of apoptosis may also be important. Recently, it has been reported that ARTS (apoptosis-related protein in the TGF-β signaling pathway) mediates apoptosis through its P-loop motif. ARTS is a member of the septin family, localizes in cellular mitochondria and plays a role in regulating apoptosis. The P-loop consensus sequence is found in the proapoptotic protein, Apaf-1/CED-4 (Yuan and Horvitz, 1992; Zou *et al*., 1997; Larisch *et al*., 2000). It is interesting that BMCC1 also possesses a P-loop motif, also suggesting its proapoptotic function.

The biological importance of BNIP2 has been reported in the neuronal system. Expression of BNIP2 is developmentally regulated during the maturation of rat brain (Zou *et al*., 1997). The recent reports suggest that expression of *BNIP2* is downregulated by the treatment of NBL cells with estrogen (Garnier *et al*., 1997), and that both estrogen and progesterone promote survival of NBL cells through the BNIP2 function during the apoptosis induced by TNF-α (Vegeto *et al*., 1999). Furthermore, BNIP2 has been identified to be a putative downstream substrate of the FGF receptor tyrosine kinase signaling and possesses GTPase-activating activity to Cdc42. Thus, BNIP2 as well as Cdc42GAP seems to play a role in controlling the intracellular signals of neuronal differentiation and apoptosis.

However, our present results show that, among the molecules with the BCH domain, only *BMCC1*, but not *BNIP2* or *Cdc42GAP*, is differentially expressed among the NBL subsets, significantly at higher levels in favorable tumors than the aggressive ones. This suggests that *BMCC1*, rather than *BNIP2* or *Cdc42GAP*, is functioning *in vivo* in favorable NBLs undergoing neuronal differentiation and/or programmed cell death. The importance of *BMCC1* in NBL cell death has also been demonstrated in the study using neuronal cell lines. The RA-induced apoptosis of CHP134 NBL cells is accompanied with increased expression of *BMCC1*, while induction of differentiation in RTBM1 cells rather decreases its mRNA level. In the former system, the RA-triggered apoptosis induced upregulation of both

Table 2 Cox regression models using *BMCC1* expression and dichotomous factors of age, *MYCN* amplification, mass screening and tumor origin ($n=98$)

Model	*Variable*	P-*value HR (95% CI)*	*Variable*	P-*value HR (95% CI)*	*Variable*	P-*value HR (95% CI)*
A	*BMCC1* exp. (log)	<0.0005 0.53 (0.40, 0.70)				
B	Age (≥1 vs <1 year)	<0.0005 7.5 (2.72, 20.7)				
C	*MYCN* (1 copy vs >1 copy)	<0.0005 0.035 (0.0099, 0.12)				
D	Mass screening (+ vs −)	<0.0005 0.028 (0.0037, 0.21)				
E	Origin (adrenal vs others)	0.072 2.7 (0.91, 8.08)				
F	*BMCC1* exp. (log)	0.007 0.55 (0.47, 0.89)	Age (≥1 vs <1 year)	0.018 3.9 (1.26, 12.0)		
G[a]	*BMCC1* exp. (log)	0.72 1.05 (0.77, 1.47)	*MYCN* (1 copy vs >1 copy)	<0.0005 0.03 (0.0071, 0.13)		
H	*BMCC1* exp. (log)	0.079 0.77 (0.57, 1.03)	Mass screening (+ vs −)	0.003 0.04 (0.0053, 0.34)		
I	*BMCC1* exp. (log)	<0.0005 0.55 (0.41, 0.74)	Origin (adrenal vs others)	0.59 1.38 (0.42, 4.46)		
J	*BMCC1* exp. (log)	0.027 0.59 (0.49, 0.96)	Age (≥1 vs <1 year)	0.014 4.1 (1.33, 12.9)	Origin (adrenal vs others)	0.403 1.5 (0.51, 5.32)

[a]One patient who had missing *MYCN* information excluded from the analysis. All variables were grouped into two categories, except *BMCC1* expression (log). HR, hazard ratio; 95% CI, confidence interval.

p21^{WAF1} and *caspase-3*, and downregulation of survivin. The downregulation and upregulation of *BMCC1* expression was also observed in the newborn mouse SCG cells undergoing NGF-induced differentiation and NGF-depletion-induced apoptosis in primary culture, respectively. Furthermore, in SCG neurons obtained from newborn transgenic mice for *BMCC1*, NGF-depletion-induced apoptosis was significantly enhanced. Thus, these results strongly suggest that *BMCC1* is stimulated or acts as a proapoptotic factor when the neuronal cell death is induced.

BMCC1 mRNA is induced at G1 phase of the cell cycle. The physiological significance of the cell cycle-dependent expression of *BMCC1* is currently unclear. However, activated Cdc42, a BMCC1-related molecule, also induces G1 cell cycle progression in quiescent Swiss 3T3 fibroblasts (Yamamoto *et al*., 1993; Olson *et al*., 1995) and upregulates E2F transcriptional activity in NIH3T3 cells to induce accumulation of cyclin D1 and hyperphosphorylation of RB protein (Gjoerup *et al*., 1998). BMCC1 may also play a role in G1-phase progression of the cell cycle via unknown mechanism.

Our statistical analysis has strongly suggested the importance of *BMCC1* expression in predicting the prognosis of NBLs. The *BMCC1* expression is upregulated in favorable NBLs and downregulated in unfavorable, advanced stages of NBLs. The similar pattern of expression in NBLs has also been reported in *TrkA* (Nakagawara *et al*., 1993, 1994; Nakagawara, 1998, 2001), *c-Ha-Ras* (Tanaka *et al*., 1998), *CD44* (Favrot *et al*., 1993) and *pleiotrophin* (Nakagawara *et al*., 1995). Here, we have added expression of BMCC1, at either mRNA or protein level, as a new prognostic indicator of favorable NBLs. Furthermore, our preliminary result has suggested that activated TrkA physically interacts with BMCC1, which in turn regulates the downstream signaling to control growth, differentiation and survival of neuronal cells (unpublished data). Therefore, BMCC1 could be a key regulator of TrkA-activation-mediated intracellular signaling pathway in favorable NBLs, that is defective in aggressive tumors such as those with *MYCN* amplification. Thus, BMCC1 might be an important molecular tool to develop new therapeutic strategy against aggressive NBLs.

Materials and methods

Patients

We studied tumors from 98 children with NBL which had been diagnosed between 1995 and 1999. In all, 55 patients were

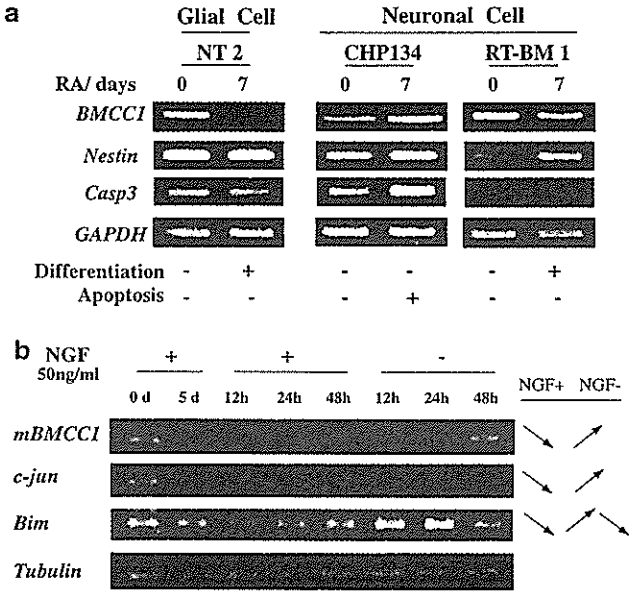

Figure 5 Expression of *BMCC1* during differentiation and apoptosis on neuronal cells. (a) The changes in *BMCC1* expression during induction of differentiation and apoptosis in neuronal cell lines. Two neuroblastoma cell lines (CHP134 and RTBM1) and teratocarcinoma cell line NT2 were treated with 5 μM all-*trans* retinoic acid (RA) or were cultured in the serum-free RPMI1640 medium for 7 days. Semiquantitative RT–PCR was performed using *BMCC1* primers and control *GAPDH* primers. (b) The changes in mRNA expression of mouse *BMCC1* during NGF-induced differentiation and NGF-depletion-induced apoptosis. Mouse superior cervical ganglion (SCG) cells were cultured with NGF for 5 days and were further cultured with or without NGF for indicated intervals (12, 24 and 48 h) (see Figure 6b, upper panels). *Tubulin* primers were used for standardization of the cDNA concentration for semiquantitative RT–PCR. *c-jun* and *Bim* were also used for positive controls.

identified by a MS program started in 1985. The selection of tumors for this study was solely based on the availability of a sufficient amount of tumor tissue, from which DNA and RNA could be prepared for the analyses described below. The diagnosis of NBL was confirmed by histologic assessment of the tumor specimen obtained at surgery according to the Shimada's classification (Shimada *et al*., 1984). The tumors were staged according to the International NBL Staging System (INSS) (Brodeur *et al*., 1993). In all, 39 tumors were stage 1, 15 stage 2, five stage 4, 10 stage 3 and 29 stage 4. The patients were treated according to the protocols previously described (Kaneko *et al*., 1998).

Tumor samples and cell lines

Fresh, frozen tumorous tissues were sent to the Division of Biochemistry, Chiba Cancer Center Research Institute, from various hospitals in Japan with informed consent from the patients' parents. All samples were obtained by surgery (or biopsy) and stored at −80°C. Studies were approved by the Institutional Review Board of the Chiba Cancer Center. Human cell lines which we used, except for COS-7, HEK 293 and HeLa cells, were cultured in the RPMI1640 medium (Nissui Pharmaceutical Co. Ltd, Tokyo, Japan) with 10% fetal bovine serum (FBS, Invitrogen Corp.) and 50 μg/ml penicillin/streptomycin (Invitrogen Corp.) at humidified 5% CO_2/95% air at 37°C. COS-7, HEK 293, and HeLa cells were grown in Dulbecco's modified Eagle's medium (DMEM) supplemented with 10% (v/v) FBS, 2 mM L-glutamine (Nissui Pharmaceutical Co. Ltd), 50 U/ml penicillin, and 50 μg/ml streptomycin.

Treatment of cell lines with RA

NT2, CHP134 and RTBM1 were seeded at a density of 1×10^6 cells per 10 cm tissue culture dish in the presence of 5 μM RA on the day of induction. The cells were grown for 7 days with substituting for culture medium with RA every other day. Total cellular RNA for preparing the RT–PCR templates was extracted after culturing for 7 days.

Cell cycle analysis

Approximately 50–70% confluent of HeLa cells were treated each by 400 μM mimosine for 18 h (G1 arrest), 2 mM thymidine for 20 h (S arrest), and 0.6 μg/ml nocodazole for 18 h (G2/M arrest). After confirmation of a synchronization of cultured cells by FACS, total RNA was extracted and the expression of *BMCC1* was examined by RT–PCR.

Northern blot analysis

Total RNA (25 μg) prepared from cell lines was electrophorased in 1% agarose-formaldehyde gels and transferred to a nylon membrane. For the hybridization probe, 1.5 kb fragment in 3′ part of *BMCC1* was used. Hybridization and washing were performed as described previously (Nagai *et al*., 2000).

Transfection and antibodies

Cells at 90% confluence in 60-mm plates were transfected with indicated plasmids using FuGENE 6 transfection reagent (Roche) for COS-7 and Lipofectamine 2000 reagent (Invitrogen) for HEK 293 cells according to their manufacturer's instructions. To generate the BMCC-1-specific antibody, rabbit antiserum was raised against the peptides individually (residues 31–59, 836–858, 993–1022, 1378–1402, 1719–1737, 2180–2209, 2693–2714) of human BMCC1. The antibody specific to C-terminal end of BMCC1 is crossreacted to human (transfectants), mouse (Neuro 2A) and rat (PC12) BMCC-1. Antiactin IgG (polyclonal) was purchased from Sigma, St Louis, MO, USA.

Semiquantitative RT–PCR

For semiquantitative RT–PCR analysis, 5 μg of total RNAs were converted to cDNA using random primers by Superscript II reverse transcriptase (Gibco-BRL). In all, 2 μl of the 100-fold dilution of cDNA was subjected to PCR. The 20 μl of PCR reaction mixture contained 1 μM forward and reverse primer specific for *BMCC1*, 250 μM deoxynucleotide triphosphates (dNTPs), 50 mM KCl, 10 mM Tris-HCl (pH 8.0), 1.5 mM $MgCl_2$ and 0.5 U Taq DNA polymerase (TAKARA, Otsu, Japan). The PCR amplification was carried out for 35 cycles (preheat at 95°C for 2 min, denature at 95°C for 15 s, annealing at 58°C for 15 s, and extension at 72°C for 20 s) in thermocycler (Perkin-Elmer Cetus, Foster City, CA, USA). The PCR products were electrophorased in 2.5% agarose gel, and visualized by UV illuminator. *BMCC1* primer sequences were as follows; forward: 5′-CGTTTATTTGCCGGTAGG AG-3′, reverse: 5′-GCTCAGGCTCTTTGGTAGGA-3′. As a control, *GAPDH* primers (forward primer; 5′-CTGCACCAA CAATATCCC-3′, reverse primer; 5′-GTAGAGACAGGG TTTCAC-3′) were also used with reduced cycle (28 cycles).

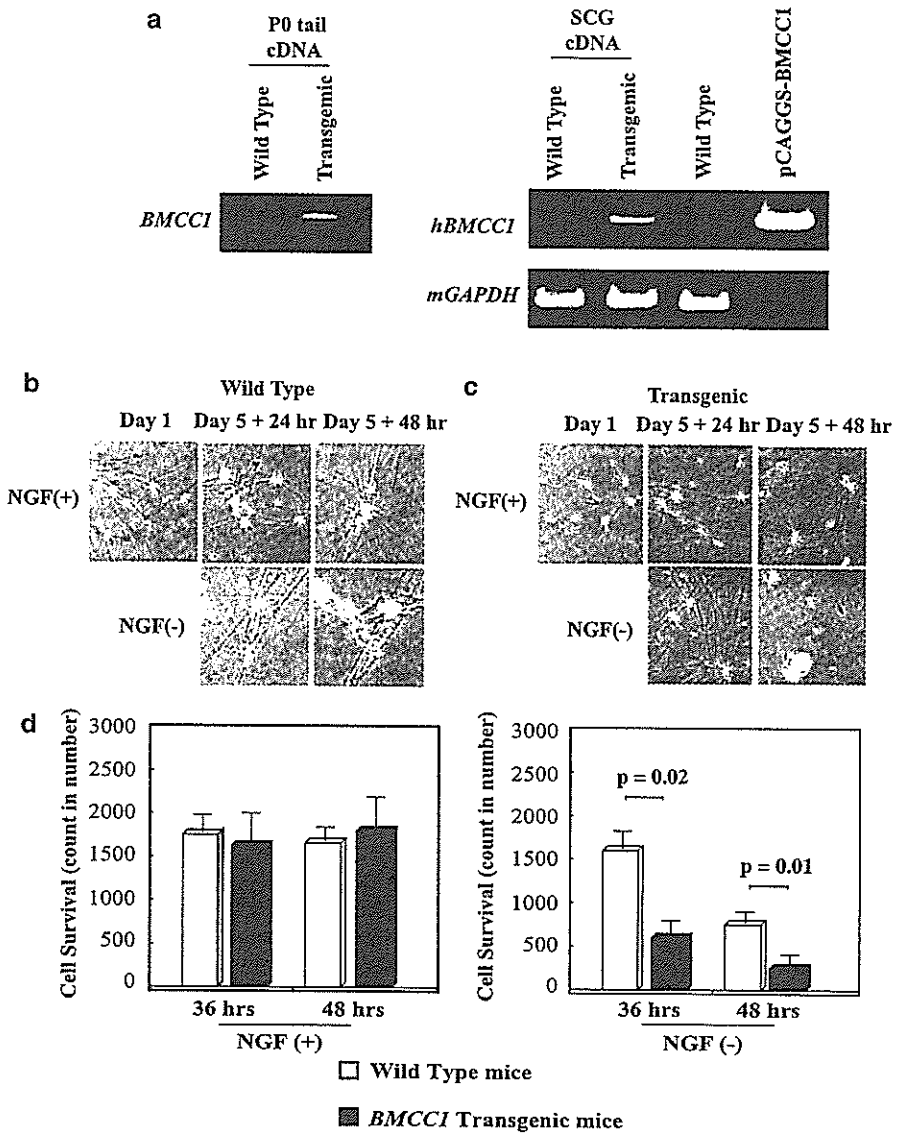

Figure 6 Increased apoptosis in superior cervical neurons obtained from newborn mice transgenic with the tyrosine hydroxylase promoter-driven human *BMCC1* in primary culture. (a) Expression of human *BMCC1* in SCG neurons obtained from *BMCC1* transgenic mice. SCG from both side of submandibular region was dissected from P_1 mice of wild-type and transgenic mice within 24 h after birth (described in Materials and methods). mRNA was purified from SCGs by using Trizol solution and RT–PCR was performed to confirm BMCC1 expression. Genotyping by PCR is shown in left panel. (b) and (c) Morphological changes in SCG neurons after treating with NGF and withdrawal of NGF. The SCG cells were obtained from wild-type (b) and BMCC1 transgenic (c) newborn mice. The cells were cultured in the presence of 50 ng/ml NGF for 5 days and were continuously treated with or without 50 ng/ml NGF for the following 2 days as described in Materials and methods. (d) Enhanced apoptosis in *BMCC1* transgenic SCG neurons after depletion of NGF. Numbers of survived SCG cells were counted at 36 and 48 h after NGF depletion. Values are shown as the means ± s.e.m. from triplicate cultures. Similar results were obtained in two additional independent experiments.

Quantitative real-time PCR analysis

For quantification of *BMCC1* in primary NBL, cDNA was synthesized with random primers by Superscript II reverse transcriptase (Gibco-BRL) from 15 μg of primary tumor total RNA. The following primers and probe were used; forward primer 5′-GGACAGTGGTCATTGGAGAACA-3′, reverse primer 5′-TTAGACCGTCCCCATAGTATCCTC-3′, probe 5′-FAM-ACATGAAGGTCATCGAGCCCTACAGG AGAG-TAMRA-3′. *GAPDH* primers and probes for control were purchased from Applied Biosystems. Quantitative real-time PCR analysis was performed by ABI7700 Prism sequence detector (Applied Biosystems), according to manufacturer's instructions using 1 × TaqMan Universal PCR Master Mix. After denaturing at 95°C for 10 min, PCR amplification followed by 40 cycles of denaturation at 95°C for 15 s and annealing/extension at 60°C for 1 min. A quantification of *BMCC1* mRNA in each samples was carried out by comparing with a standard curve, which was generated by reacting the plasmid containing *BMCC1*. Furthermore, *GAPDH* mRNA quantification was also performed for a standardization of the initial RNA content of each samples.

Exon prediction and bioinformatics

BLAST search against genome database revealed that 5′-region of *Nbla00219* was matched to the genome sequence of a

BAC clone RP11-146P9 (GenBank accession no. AL161625). We used GENESCAN algorithm (Burge and Karlin, 1997, 1998), and FGENESH algorithm (Solovyev and Salamov, 1999) to predict ORF from the genome sequence, and designed primers from each deduced exons. Using these primers and primers from 5′-region of *Nbla00219* cDNA, RT–PCR was performed to confirm the real exons. All PCR products were sequenced by the ABI automatic DNA sequencer (Perkin-Elmer Cetus) and resulting sequence were assembled to the full-length *BMCC1* cDNA. Bioinformatic analysis was performed using the PSORTII algorithm (Horton and Nakai, 1996), the SOPM algorithm and the TM pred algorithm against the predicted amino-acid sequences of *BMCC1*.

In situ *hybridization*
Section *in situ* hybridization was carried out as described previously (Takihara *et al*., 1997). The embryos were collected from pregnant females, and the morning the vaginal plug was detected was recorded as E0.5. A riboprobe was synthesized with digoxygenin-UTP and T3 or T7 polymerase (Roche Molecular Biochemicals). The alkaline phosphatase reaction was performed with NBT-BCIP (Roche Molecular Biochemicals). The riboprobes used for the section *in situ* hybridization were transcripts of the genomic DNA fragments of the *BMCC1* gene, a 835 bp PCR product of exon 3: the primers used are 5′-GAGATACTGGAGTTAGAAGAAG-3′ and 5′-TTCGGTCTTGGCTTTCTGGGTC-3′.

Immunohistochemistry
NBLs of favorable histology (Shimada system) without *MYCN* amplification and those of unfavorable histology with *MYCN* amplification were analysed. Anti-BMCC1 antibody was diluted to 1:50 and applied to the immunostaining. After deparaffinization, the sections were treated with 0.05% pronase solution for 5 min at room temperature. The biotin–streptoavidin method (Nichirei, Tokyo, Japan) was performed, and the reaction was visualized with diaminobenzidine solution.

Generation of BMCC1 transgenic mice
The full-length cDNA encoding human *BMCC1* was subcloned into the *Eco*RI site of the multicloning site region of the transgenic expression vector pCAGGS. The resulting plasmid, pCAGGS-*BMCC1*, was digested by *Alw44*I to isolate the transgenic cassette consisting of the CMV enhancer, the chicken *β-actin* promoter, the *BMCC1* cDNA, and the rabbit *β-globin* poly(A) sequence. The isolated region was purified for pronuclear injection into mouse embryos from FVB mice (Charles River Japan Inc.). Mouse embryos (fertilized one-cell zygotes) were injected and implanted in female CD-1 mice (Charles River Japan Inc.) at Japan SLC Inc. (Shizuoka, Japan). *BMCC1* transgenic mice were identified by slot blot analysis using genomic DNA prepared from mouse tails. *BMCC1*-positive founder transgenic mice then were backcrossed at least three times with C57BL/6 mice. Positive mice comprising the F_4 generation were subjected to SCG analyses.

Primary culture of newborn mice SCG cells
Primary cultures of sympathetic neurons were generated from dissociated SCG of postnatal-day 1 wild-type and transgenic mice as described previously (Lee *et al*., 1980). The cells were plated onto collagen-coated 24-well dishes at a density of around two ganglia per well and maintained in Modified Eagle's Medium supplemented with 10% heat-inactivated donor serum and 50 ng of mouse NGF per ml. A mixture of uridine and 5-fluorodeoxyuridine (10 μM each) was added on the following day to eliminate non-neuronal cells.

Statistical analysis
The Student's *t*-tests were used to explore possible associations between *BMCC1* expression and other factors, such as age. Since the values of the *BMCC1* expression were skewed, a log transformation was used to achieve the normality when using *t*-test and Cox regression. The distinction between high and low levels of *BMCC1* was based on the median value of the real-time PCR data (low, *BMCC1* <0.86 d.u.; high, *BMCC1* $\geqslant 0.86$ d.u.), regardless of tumor stage, *MYCN* copy, or survival. Kaplan–Meier survival curves were calculated, and survival distributions were compared using the log-rank test. Cox regression models were used to explore associations between *BMCC1*, age, *MYCN*, MS, origin and survival. Statistical significance was declared if the *P*-value was <0.05. Statistical analysis was performed using Stata 6.0. (Stata Corp. 1998. Stata Statistical Software: Release 6.0 College Station, TX: Stata Corporation).

Acknowledgements

We thank Shigeyuki Furuta, Shiho Hamano, Hiroyuki Inuzuka, Aiko Morohashi for technical assistance, Masayuki Fukumura, Toshihide Kanamori and Mika Kimura for helping full-length cDNA cloning, and Shigeru Sakiyama for encouragement. This work was supported in part by a Grant-in-Aid for the 2nd Term Comprehensive 10-Year Strategy for Cancer Control from the Ministry of Health, Labour and Welfare of Japan (AN), and by Grant-in-Aid for Scientific Research (B) (AN) and for Scientific Research on Priority Areas (2) 'Medical Genome Science' (MO, EI, AN) from the Ministry of Education, Culture, Sports, Science and Technology of Japan, and by a fund from Hisamitsu Pharmaceutical Co. Inc. (AN). We also thank following hospitals and departments for providing surgical samples: First Department of Surgery, Hokkaido University School of Medicine; Department of Pediatrics, National Sapporo Hospital; Department of Pediatric Surgery, Tohoku University School of Medicine; Department of Surgery, Gunma Children's Medical Center; Department of Pediatrics, Pediatric Surgery and General Surgery, Jichi Medical University; Department of Hematology and Oncology, Saitama Children's Medical Center; Department of Pediatrics, Juntendo University School of Medicine; Department of Surgery, Kiyose Metropolitan Children's Hospital; Department of Surgery and Pathology, Chiba Children's Hospital; Department of Pediatric Surgery, Chiba University School of Medicine; Department of Pediatric Surgery, Kimitsu Central Hospital; Department of Pediatric Surgery, Niigata University School of Medicine; Department of Pediatrics and Pediatric Surgery, Aichi Medical University; Department of Pediatrics, Kyoto Prefectural Medical University; Tumor Board, Hyogo Children's Hospital; Department of Pediatrics and Pediatric Surgery, Kagoshima University School of Medicine; Department of Pediatric Surgery, Showa University School of Medicine; Department of Pediatrics, Oita University School of Medicine; Department of Pediatric Surgery, Ohta General Hospital; Department of Pediatrics, Ichinomiya City Hospital; Department of Pediatric Surgery, Osaka City General Hospital; Department of Pediatrics, Nihon University School of Medicine Itabashi Hospital; Department of Pediatric Surgery, University of Tsukuba School of Medicine.

References

Bagrodia S, Derijard B, Davis RJ, Cerione RA. (1995). *J Biol Chem* **270**: 27995–27998.

Bazenet CE, Mota MA, Rubin LL. (1998). *Proc Natl Acad Sci USA* **95**: 3984–3989.

Boyd JM, Malstrom S, Subramanian T, Venkatesh LK, Schaeper U, Elangovan B *et al.* (1994). *Cell* **79**: 341–351.

Brodeur GM, Pritchard J, Berthold F, Carlsen NL, Castel V, Castelberry RP *et al.* (1993). *J Clin Oncol* **11**: 1466–1477.

Brodeur GM, Seeger RC, Schwab M, Varmus HE, Bishop JM. (1984). *Science* **224**: 1121–1124.

Burge C, Karlin S. (1997). *J Mol Biol* **268**: 78–94.

Burge CB, Karlin S. (1998). *Curr Opin Struct Biol* **8**: 346–354.

Cahill MA, Peter ME, Kischkel FC, Chinnaiyan AM, Dixit VM, Krammer PH *et al.* (1996). *Oncogene* **13**: 2087–2096.

Caron H. (1995). *Med Pediatr Oncol* **24**: 215–221.

Chuang TH, Hahn KM, Lee JD, Danley DE, Bokoch GM. (1997). *Mol Biol Cell* **8**: 1687–1698.

Coso OA, Chiariello M, Yu JC, Teramoto H, Crespo P, Xu N *et al.* (1995). *Cell* **81**: 1137–1146.

Evans AE, Gerson J, Schnaufer L. (1976). *Natl Cancer Inst Monogr* **44**: 49–54.

Favrot MC, Combaret V, Lasset C. (1993). *N Engl J Med* **329**: 1965.

Garcia I, Martinou I, Tsujimoto Y, Martinou JC. (1992). *Science* **258**: 302–304.

Garnier M, Di Lorenzo D, Albertini A, Maggi A. (1997). *J Neurosci* **17**: 4591–4599.

Gjoerup O, Lukas J, Bartek J, Willumsen BM. (1998). *J Biol Chem* **273**: 18812–18818.

Gooding LR, Aquino L, Duerksen-Hughes PJ, Day D, Horton TM, Yei SP *et al.* (1991). *J Virol* **65**: 3083–3094.

Hashimoto S, Ishii A, Yonehara S. (1991). *Int Immunol* **3**: 343–351.

Hockenbery D, Nunez G, Milliman C, Schreiber RD, Korsmeyer SJ. (1990). *Nature* **348**: 334–336.

Horton P, Nakai K. (1996). *Proc Int Conf Intell Syst Mol Biol* **4**: 109–115.

Islam A, Kageyama H, Takada N, Kawamoto T, Takayasu H, Isogai E *et al.* (2000). *Oncogene* **19**: 617–623.

Juo P, Kuo CJ, Reynolds SE, Konz RF, Raingeaud J, Davis RJ *et al.* (1997). *Mol Cell Biol* **17**: 24–35.

Kaneko M, Nishihira H, Mugishima H, Ohnuma N, Nakada K, Kawa K *et al.* (1998). *Med Pediatr Oncol* **31**: 1–7.

Kozak M. (1987). *Nucl Acids Res* **15**: 8125–8148.

Larisch S, Yi Y, Lotan R, Kerner H, Eimerl S, Tony Parks W *et al.* (2000). *Nat Cell Biol* **2**: 915–921.

Lee VM, Shelanski ML, Greene LA. (1980). *Neuroscience* **5**: 2239–2245.

Lenczowski JM, Dominguez L, Eder AM, King LB, Zacharchuk CM, Ashwell JD. (1997). *Mol Cell Biol* **17**: 170–181.

Low BC, Seow KT, Guy GR. (2000). *J Biol Chem* **275**: 37742–37751.

Moasser MM, Khoo KS, Maerz WJ, Zelenetz A, Dmitrovsky E. (1996). *Differentiation* **60**: 251–257.

Nagai M, Ichimiya S, Ozaki T, Seki N, Mihara M, Furuta S *et al.* (2000). *Int J Oncol* **16**: 907–916.

Nakagawara A. (1998). *Hum Cell* **11**: 115–124.

Nakagawara A. (2001). *Cancer Lett* **169**: 107–114.

Nakagawara A, Arima-Nakagawara M, Scavarda NJ, Azar CG, Cantor AB, Brodeur GM. (1993). *N Engl J Med* **328**: 847–854.

Nakagawara A, Azar CG, Scavarda NJ, Brodeur GM. (1994). *Mol Cell Biol* **14**: 759–767.

Nakagawara A, Milbrandt J, Muramatsu T, Deuel TF, Zhao H, Cnaan A *et al.* (1995). *Cancer Res* **55**: 1792–1797.

Nakamura Y, Ozaki T, Ichimiya S, Nakagawara A, Sakiyama S. (1998). *Biochem Biophys Res Commun* **243**: 722–726.

Ohira M, Morohashi A, Inuzuka H, Shishikura T, Kawamoto T, Kageyama H *et al.* (2003a). *Oncogene* **22**: 5525–5536.

Ohira M, Morohashi A, Nakamura Y, Isogai E, Furuya K, Hamano S *et al.* (2003b). *Cancer Lett* **197**: 63–68.

Olson MF, Ashworth A, Hall A. (1995). *Science* **269**: 1270–1272.

Oltvai ZN, Milliman CL, Korsmeyer SJ. (1993). *Cell* **74**: 609–619.

Seimiya H, Mashima T, Toho M, Tsuruo T. (1997). *J Biol Chem* **272**: 4631–4636.

Shimada H, Chatten J, Newton Jr WA, Sachs N, Hamoudi AB, Chiba T *et al.* (1984). *J Natl Cancer Inst* **73**: 405–416.

Solovyev VV, Salamov AA. (1999). *Nucl Acids Res* **27**: 248–250.

Subramanian T, Boyd JM, Chinnadurai G. (1995). *Oncogene* **11**: 2403–2409.

Takihara Y, Tomotsune D, Shirai M, Katoh-Fukui Y, Nishii K, Motaleb MA *et al.* (1997). *Development* **124**: 3673–3682.

Tanaka T, Sugimoto T, Sawada T. (1998). *Cancer* **83**: 1626–1633.

Vegeto E, Pollio G, Pellicciari C, Maggi A. (1999). *FASEB J* **13**: 793–803.

White E, Sabbatini P, Debbas M, Wold WS, Kusher DI, Gooding LR. (1992). *Mol Cell Biol* **12**: 2570–2580.

Whitfield J, Neame SJ, Paquet L, Bernard O, Ham J. (2001). *Neuron* **29**: 629–643.

Yamamoto M, Marui N, Sakai T, Morii N, Kozaki S, Ikai K *et al.* (1993). *Oncogene* **8**: 1449–1455.

Yuan J, Horvitz HR. (1992). *Development* **116**: 309–320.

Zhang B, Zhang Y, Collins CC, Johnson DI, Zheng Y. (1999). *J Biol Chem* **274**: 2609–2612.

Zhang B, Zheng Y. (1998). *J Biol Chem* **273**: 25728–25733.

Zhang S, Han J, Sells MA, Chernoff J, Knaus UG, Ulevitch RJ *et al.* (1995). *J Biol Chem* **270**: 23934–23936.

Zhou YT, Soh UJ, Shang X, Guy GR, Low BC. (2002). *J Biol Chem* **277**: 7483–7492.

Zou H, Henzel WJ, Liu X, Lutschg A, Wang X. (1997). *Cell* **90**: 405–413.

FEBS Letters 580 (2006) 627–632

High expression of *N*-acetylglucosaminyltransferase V in favorable neuroblastomas: Involvement of its effect on apoptosis

Kei-ichiro Inamori[a], Jianguo Gu[a,*], Miki Ohira[b], Atsushi Kawasaki[b], Yohko Nakamura[b], Takatoshi Nakagawa[c], Akihiro Kondo[c], Eiji Miyoshi[a], Akira Nakagawara[b], Naoyuki Taniguchi[a]

[a] *Department of Biochemistry, Osaka University Graduate School of Medicine, 2-2 Yamadaoka, Suita, Osaka 565-0871, Japan*
[b] *Division of Biochemistry, Chiba Cancer Center Research Institute, 666-2 Nitona, Chuoh-ku, Chiba 260-8717, Japan*
[c] *Department of Glycotherapeutics, Osaka University Graduate School of Medicine, 2-2 Yamadaoka, Suita, Osaka 565-0871, Japan*

Received 1 December 2005; revised 27 December 2005; accepted 29 December 2005

Available online 5 January 2006

Edited by Laszlo Nagy

Abstract Neuroblastoma (NBL), derived from the sympathetic precursor cells, is one of the most common pediatric solid tumors. The expression of *N*-acetylglucosaminyltransferase V and IX (GnT-V and GnT-IX) mRNA in 126 primary NBLs were quantitatively analyzed and higher expression levels of GnT-V were found to be associated with favorable stages (1, 2 and 4s). Conversely, the downregulation of GnT-V expression by small interfering RNA resulted in a decrease in the susceptibility to cell apoptosis induced by retinoic acid in NBL cells accompanied by morphological change. These results suggest that GnT-V is associated with prognosis by modulating the sensitivity of NBLs to apoptosis.

Keywords: Neuroblastoma; GnT-V; GnT-IX; Retinoic acid; Apoptosis

1. Introduction

Aberrant glycosylation occurs in nearly all types of cancers, and has been implicated in the malignancy that is characteristic of the disease [1]. *N*-acetylglucosaminyltransferase V (GnT-V) is one of the most relevant glycosyltransferases to tumor invasion and metastasis, and catalyzes the formation of β1,6GlcNAc branching on *N*-glycans, which is closely associated with malignant transformations [2–6]. Recently, our group and Pierce's group independently reported on a new *N*-acetylglucosaminyltransferase IX (GnT-IX, also referred to as GnT-VB), a GnT-V homolog, that is specifically expressed in the brain [7,8]. GnT-IX transcripts are exclusively expressed in the brain and testis, while GnT-V is expressed ubiquitously in human and mouse tissues. Since both glycosyltransferases are expressed in the mouse brain in a region-specific manner (unpublished data), it is possible that they may have discrete biological functions in the brain. On the other hand, GnT-V and GnT-IX are both highly expressed in both the adult and fetal brain [7,9], as well as in several human neuroblastoma (NBL) cell lines (this study and unpublished data). This prompted us to examine the expression of GnT-V and GnT-IX in primary NBL tissues.

NBL is a tumor derived from primitive cells of the sympathetic nervous system and is the most common solid tumor in childhood [10]. Interestingly, most NBLs in infants regress spontaneously or mature into a benign ganglioneuroma. These tumors usually express high levels of TrkA, and as a result, have a tendency to either undergo apoptosis or differentiation, depending on whether nerve growth factor is present or absent in their microenvironment. On the other hand, in most patients over 1 year of age who have metastatic disease, the tumor grows aggressively and their prognosis is usually poor.

In this study, we carried out a quantitative analysis of the gene expression of these glycosyltransferases by real-time PCR, and the findings indicate that a higher expression of GnT-V is correlated with a favorable prognosis for NBL patients. Furthermore, to explore the underlying molecular mechanism, we devised a knockdown approach, in which small interfering RNA (siRNA)-directed against GnT-V mRNA was used to investigate the susceptibility to cell apoptosis induced by retinoic acid in NBL cells. The results clearly showed that the expression levels of GnT-V are associated with a favorable prognosis, possibly through sensitizing to apoptotic signals.

2. Materials and methods

2.1. RNA isolation from primary NBLs

Fresh, frozen tumor tissues were sent to the Division of Biochemistry, Chiba Cancer Center Research Institute, from various hospitals in Japan with informed consent from the patients' parents. All samples were obtained by surgery or biopsy and had been stored at 80 °C. The RNA samples obtained from 126 patients with NBL were subjected to semiquantitative and quantitative real-time reverse transcription-PCR (RT-PCR) analyses. All of the patients were diagnosed clinically as well as pathologically and were tested for DNA ploidy, MYCN amplification, and TrkA expression. The tumors were staged according to the criteria of the International Neuroblastoma Staging System [11].

2.2. Semiquantitative RT-PCR analysis of primary NBLs

The preparation of total RNA from NBL tissues and the synthesis of the first-strand cDNA were performed as described previously [12]. The cDNA was diluted to a 1:20 solution and then amplified in a final

*Corresponding author. Fax: +81 6 6879 3429.
E-mail address: jgu@biochem.med.osaka-u.ac.jp (J. Gu).

Abbreviations: NBL, neuroblastoma; GnT-V, *N*-acetylglucosaminyltransferase V; GnT-IX, *N*-acetylglucosaminyltransferase IX; RT, reverse transcription; PARP, poly(ADP-ribose) polymerase

0014-5793/$32.00
doi:10.1016/j.febslet.2005.12.089

volume of 10 μl of reaction mixture containing 200 μM of dNTPs, 1× PCR buffer, 0.5 μM of each primer and 0.2 U of rTaq DNA polymerase (Takara Bio, Ohtsu, Japan). The following primer sets were used: GnT-V, 5′-GACCTGCAGTTCCTTCTTCG-3′ and 5′-CCATGGCAGAAGTCCTGTTT-3′; GnT-IX, 5′-CATGGCACCGTGTACTAC-3′ and 5′-TCTGGAGCTCTGCAGAAG-3′. PCR templates were standardized by their GAPDH expression before performing the RT-PCR experiments.

2.3. Quantitative real-time PCR analysis of primary NBLs

2 μl of cDNA prepared as above, either a 100-fold dilution for GnT-V or a 20-fold dilution for GnT-IX, was amplified in a volume of 20 μl with Assay-on-Demand Gene Expression Products (Applied Biosystems) consisting of primers and a TaqMan probe (Assay ID: GnT-V, Hs00159136_m1; GnT-IX, Hs01586304_g1). The thermal cycling conditions and the normalization of the data using GAPDH expression were performed as described previously [12]. All experiments were carried out in triplicate for each data point.

2.4. Assay of GlcNAc transferase activity

The activities of GnT-V and GnT-III in whole cell lysates or microsomal fractions were determined using a pyridylaminated biantennary sugar chain as an acceptor substrate, as described previously [7,13].

2.5. Construction of siRNA vector and retroviral infection

Small interfering oligonucleotides specific for GnT-V were designed on the Takara Bio website (http://www.takara-bio.co.jp/) and the oligonucleotide sequences used in the construction of the siRNA vector were as follows: 5′-GATCCGTTCATTGGCGGAAATTCGTTTCAAGAGAACGAATTTCCGCCAATGAACTTTTTTAT-3′ and 5′-CGATAAAAAAGTTCATTGGCGGAAATTCGTTCTCTTGAAACGAATTTCCGCCAATGAACG-3′. The oligonucleotides were annealed and then ligated into *BamHI/ClaI* sites of the pSINsi-hU6 vector (Takara Bio). A retroviral supernatant was obtained by transfection of human embryonic kidney 293 cells using a Retrovirus Packaging Kit Ampho (Takara Bio) according to the manufacturer's protocol. CHP134 cells, a human NBL cell line, were infected with the viral supernatant, and the cells were then selected with 0.5 mg/ml G418 for 2–3 weeks. Stable GnT-V-knockdown clones were selected and confirmed by GnT-V activity and gene expression. Quantitative real-time PCR analyses of GnT-V mRNA expression in these clones were performed with a Smart Cycler II System and the SYBR premix Taq (Takara Bio). RT was carried out at 42 °C for 10 min, followed by 95 °C for 2 min using random primers, followed by PCR for 50 cycles at 95 °C for 5 s and 60 °C for 20 s with the following primers: 5′-AAGCAGGTGTGCCAGGAGAG-3′ and 5′-GTCAAAGGAGGGCACCAGGA-3′. Normalization of the data was performed using the GAPDH mRNA levels.

2.6. Analysis of retinoic acid-induced apoptosis

Parent, mock, and GnT-V-knockdown CHP134 cells were plated on 10 cm culture dishes at 5×10^5 cells in RPMI1640 supplemented with 10% fetal bovine serum, 100 U/ml penicillin, and 0.1 mg/ml streptomycin. After incubation for 24 h, the conditioned media were changed with fresh medium containing various concentrations of all-*trans* retinoic acid (Sigma). The cells were washed twice with PBS and harvested at the indicated times. Retinoic acid-induced apoptosis was estimated by detecting the cleavage of poly ADP-ribose polymerase (PARP) in whole cell lysates by Western blot analysis using a human specific anti-cleaved PARP (Asp214) antibody (Cell Signaling Technology). As a loading control, anti-ERK1/2 (p44/42 MAP Kinase Antibody, Cell Signaling Technology) was used.

2.7. Viability assay of retinoic acid-treated cells

The parent, mock, and GnT-V-knockdown CHP134 cells were seeded on a 96-well plate at 3×10^3 cells/well for 24 h prior to the retinoic acid treatment. The cells were then incubated with or without retinoic acid at the indicated concentrations for 3 days. Cell viability was assayed using a Cell Counting Kit-8 (Dojindo, Kumamoto, Japan) according to the manufacture's instructions. All experiments were carried out in triplicate for each data point.

3. Results

3.1. Association between higher expression levels of GnT-V mRNA and favorable prognosis in primary NBLs

To assess the association between GnT-V or GnT-IX mRNA expression and the prognosis of the NBLs, we first performed semiquantitative RT-PCR analyses using 16 favorable and 16 unfavorable NBLs. As shown in Fig. 1, GnT-V was preferentially expressed in most of the favorable NBLs, while no obvious difference in GnT-IX expression was found between favorable and unfavorable NBLs. Table 1 shows quantitative data for GnT-V and GnT-IX mRNA in 126 primary NBLs with tumor stages (1, 2, 4s versus 3, 4). GnT-V expression was significantly increased in NBLs at favorable stages ($P = 0.021$), and was correlated well with higher expression of TrkA ($P = 0.010$). On the other hand, GnT-IX expression was marginally associated with the stages.

3.2. GnT-V activities in various human NBL cell lines

To determine whether the expression level of GnT-V is also increased in NBL cells, the activities of GnT-V in various human NBL cell lines were examined. As shown in Fig. 2A, each cell line expressed GnT-V activity at distinct levels. The CHP134 cells showed the highest GnT-V activity among the 10 NBL cell lines used in this study. It is known that the cell line is highly sensitive to the induction of apoptosis by all-*trans* retinoic acid [14,15]. In fact, it is thought that favorable NBLs usually express higher levels of TrkA, and tend to regress spontaneously due to apoptosis. As shown in Fig. 2B, in CHP134 cells that had been treated with retinoic acid at a concentration of 1 μM or 5 μM, PARP cleavage, a marker for apoptosis, occurred, which is one of the main cleavage targets of caspase-3

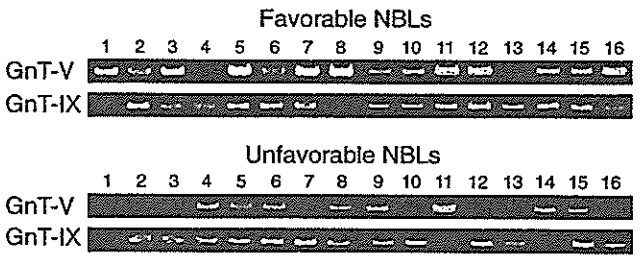

Fig. 1. Semiquantitative RT-PCR analysis of favorable and unfavorable subsets of NBL. Sixteen favorable cases were in stage 1 with no MYCN amplification and a high TrkA expression, while 16 unfavorable cases were in stage 3 or 4 with MYCN amplification and a low TrkA expression.

Table 1
Association of tumor stages and *TrkA* expression in NBL patients with GnT-V or GnT-IX mRNA expression levels

	n	GnT-V[a]	*P*	GnT-IX[a]	*P*
Tumor stage					
1, 2, 4s	57	2.23 ± 0.29	0.021	1.78 ± 0.25	0.21
3, 4	69	1.48 ± 0.16		2.23 ± 0.25	
TrkA expression					
High	59	2.11 ± 0.27	0.010	1.86 ± 0.17	0.75
Low	48	1.33 ± 0.13		1.98 ± 0.34	

[a]Means ± S.E.M.

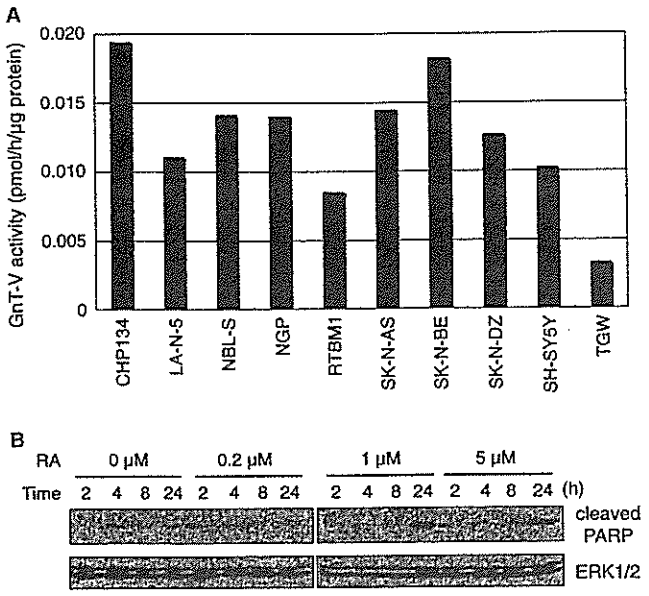

Fig. 2. GnT-V activities in various NBL cell lines and retinoic acid-induced apoptosis of CHP134 cells. (A) GnT-V activity of each of the NBL cells was measured using a whole cell lysate as an enzyme source. (B) Western blot of whole cell lysate of CHP134 cells. Cell apoptosis was observed by staining of cleaved PARP after treatment of retinoic acid (RA) at indicated concentrations and times. The expression levels of ERK1/2 were confirmed as a loading control.

in vivo [16,17]. Thus, we chose this cell line for further analysis of the effects of GnT-V on apoptosis.

3.3. Knockdown of GnT-V expression in CHP134 cells

We prepared a retroviral siRNA vector containing a small hairpin construct capable of generating a duplex RNAi oligonucleotide corresponding to human GnT-V. After retroviral infection, CHP134 cells were selected based on their resistance to G418, and clones with decreased GnT-V activities were chosen. The GnT-V activities were effectively downregulated by 80%, compared with those in parent or mock cells (Fig. 3A), while GnT-III activity, as a control, showed no significant changes between those cells. A quantitative real-time PCR analysis also indicated the downregulation of RNAi-directed GnT-V mRNA expression in these cells (Fig. 3B). It is noteworthy that the cells in GnT-V-knockdown clones showed more spreading on the culture dishes, rather than the spindle shapes of the parent and mock cells (Fig. 4), suggesting that GnT-V may affect cellular cytoskeletal formation. In fact, Guo et al. reported that the overexpression of GnT-V in human HT1080 cells resulted in a decrease in cell adhesion on fibronectin [18].

3.4. Decreased susceptibility to retinoic acid-induced apoptosis in GnT-V-knockdown cells

To evaluate the effects of GnT-V expression on susceptibility to apoptosis induction in CHP134 cells, we examined cell viabilities in the presence of retinoic acid. After treatment with different concentrations of retinoic acid, we found that GnT-V-knockdown cells (KD1 and KD2 in Fig. 5A) had a tendency to be resistant to stimulation by retinoic acid. We further assessed the apoptosis level in retinoic acid-treated cells by PARP cleavage. The GnT-V-knockdown cells showed dramatically reduced levels of PARP cleavage (Fig. 5B). Collectively, these results suggest that GnT-V may sensitize cells to apoptotic signals, which partly contribute to the favorable prognosis of NBL.

4. Discussion

Previous studies demonstrated that an increased amount of β1,6-branched oligosaccharides, formed by the action of GnT-V, are correlated with metastatic potential [2], and this has been shown to be a marker of tumor progression in human breast and colon neoplasia [19], and a prognostic marker in human colorectal carcinoma [20,21]. However, it is not always the case, as evidenced by the fact that Dosaka-Akita et al. reported that the lower expression of GnT-V is associated with a shorter survival and a poor prognosis in non-small cell lung cancers [22]. The present study also suggested that a higher expression of GnT-V is related to a favorable prognosis in NBLs.

GnT-V and GnT-IX, two closely related glycosyltransferases, are expressed in both the adult and fetal brain [7,9]. GnT-V expression is upregulated in E9.5 embryos, and is then

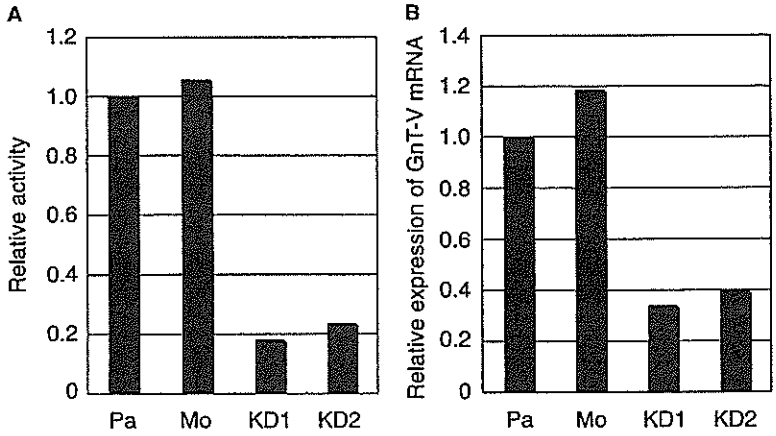

Fig. 3. Enzyme activities and mRNA expression levels in siRNA-mediated GnT-V-knockdown cells. (A) GnT-V activities of GnT-V-knockdown CHP134 cells. The microsomal fraction was used as an enzyme source in the assay. (B) mRNA expression of GnT-V in knockdown cells. Quantitative analysis was performed by real-time PCR. Pa, parent cells; Mo, mock cells; KD1 and KD2, GnT-V-knockdown cells.

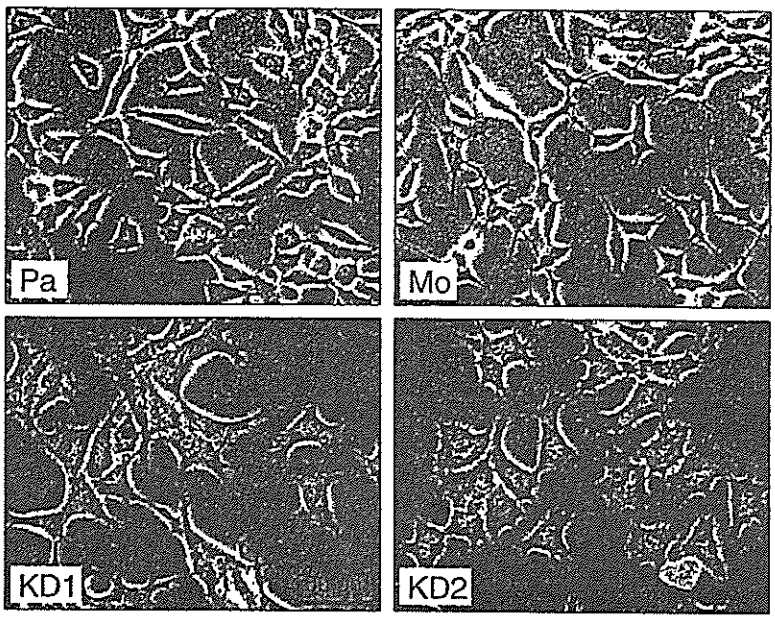

Fig. 4. Morphological changes in GnT-V-knockdown cells. Parent (Pa), mock (Mo), and GnT-V-knockdown CHP134 cells (KD1, KD2) were plated on culture dishes and incubated for 24 h in culture media. Cell shapes were observed by phase contrast microscopy.

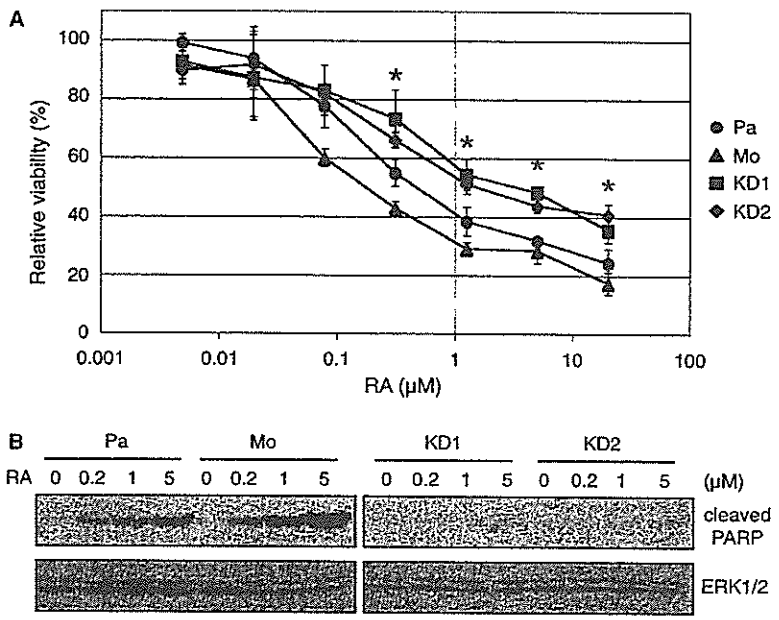

Fig. 5. Cell viabilities and PARP cleavage in retinoic acid-treated GnT-V-knockdown cells. Cell viabilities of parent (Pa), mock (Mo), and GnT-V-knockdown cells (KD1, KD2) were performed as described in Section 2 (A). Cells were treated with retinoic acid at the indicated concentrations for 3 days. $^{*}P < 0.05$. (B) Western blot of cleaved PARP in a cell lysate using an anti-cleaved PARP antibody. Cells were harvested for analysis 24 h after retinoic acid-treatment.

restricted to regions comprised of several specialized epithelial cell layers and the neuroepithelium of the developing central nervous system [9]. On the other hand, GnT-IX is dominantly expressed in the human and mouse brain [7,23]. Thus, we attempted to examine the expressions of GnT-V and GnT-IX in primary NBL tissues.

The frequent gain of the chromosome 17q has been reported to be associated with a poor prognosis [24], and the preferential gain of the region from 17q22-qter indicated a dosage effect that provides a selective advantage to be aggressive NBLs [25]. The gene responsible for the selective advantage is unknown, but a candidate gene that is a member of the inhibitor of apoptosis proteins, survivin, which is mapped to 17q25, has been reported [14]. Although the GnT-IX gene is also mapped to 17q25 [7], an unequivocal correlation with prognosis was not observed in this study. Interestingly, a significant association between expression levels of GnT-V mRNA and the prognosis of 126 NBL patients was observed by real-time PCR analysis. Several human NBL cell lines also consistently express GnT-V. To understand the molecular mechanism associated with the

higher expression levels of GnT-V in the favorable prognosis of NBLs, we selected CHP134 cells as a cell model. Since the cell line is highly sensitive to retinoic acid-induced apoptosis [14,15], we compared the effects of retinoic acid on apoptosis between parent cells and GnT-V-knockdown cells.

In fact, GnT-V-knockdown cells showed a tendency to escape from retinoic acid-induced apoptosis, as confirmed by a cell viability assay and the extent of cleaved PARP, supporting the notion that a higher expression of GnT-V is correlated with a favorable prognosis of NBLs. It is noteworthy that a prominent morphological alteration with increased spreading was observed in the GnT-V-knockdown cells. The altered characteristic of GnT-V-knockdown CHP134 cells observed in this study is consistent with those of previous studies [3,18,26,27]. The overexpression of GnT-V enhances the metastatic potential in several cell types with reduced cell-matrix adhesion and increased motility [3,18,26]. Furthermore, GnT-V expression in human glioma cell line U-373 MG sensitizes these cells to drag-induced apoptosis [28]. Conversely, GnT-V null mouse embryonic fibroblasts exhibited an enhanced adhesion and spreading with associated reduced cell migration [27]. In addition, no significant effect of GnT-V overexpression was observed on apoptotic behavior in fibrosarcoma HT1080 cells, a fibroblast cell line, but a similar phenotypic change with regard to adhesion and migration has been reported [18]. In general, the adhesion of epithelial cells to extracellular matrices is weaker than that of fibroblast cells, and such adhesion is thought to be synergized with the signals of growth factor receptors for modulating cell proliferation and apoptosis. Therefore, we speculate that the GnT-V-induced decrease in cell adhesion could be a plausible factor responsible for the favorable prognosis in NBLs.

In conclusion, a correlation between higher expression levels of GnT-V with a favorable prognosis of NBL patients was found, and GnT-V may cause these tumors to regress by increasing their susceptibility to apoptosis.

Acknowledgments: This work was supported a Grant-in-Aid for Scientific Research (S) No. 13854010 from the Japan Society for the promotion of Science and by the 21st Century COE Program by the Ministry of Education, Science, Culture, Sports and Technology in Japan.

References

[1] Hakomori, S. (2002) Glycosylation defining cancer malignancy: new wine in an old bottle. Proc. Natl. Acad. Sci. USA 99, 10231–10233.

[2] Dennis, J.W., Laferte, S., Waghorne, C., Breitman, M.L. and Kerbel, R.S. (1987) Beta 1–6 branching of Asn-linked oligosaccharides is directly associated with metastasis. Science 236, 582–585.

[3] Demetriou, M., Nabi, I.R., Coppolino, M., Dedhar, S. and Dennis, J.W. (1995) Reduced contact-inhibition and substratum adhesion in epithelial cells expressing GlcNAc-transferase V. J. Cell. Biol. 130, 383–392.

[4] Granovsky, M., Fata, J., Pawling, J., Muller, W.J., Khokha, R. and Dennis, J.W. (2000) Suppression of tumor growth and metastasis in Mgat5-deficient mice. Nat. Med. 6, 306–312.

[5] Saito, T., Miyoshi, E., Sasai, K., Nakano, N., Eguchi, H., Honke, K. and Taniguchi, N. (2002) A secreted type of beta 1,6-*N*-acetylglucosaminyltransferase V (GnT-V) induces tumor angiogenesis without mediation of glycosylation: a novel function of GnT-V distinct from the original glycosyltransferase activity. J. Biol. Chem. 277, 17002–17008.

[6] Ihara, S., Miyoshi, E., Ko, J.H., Murata, K., Nakahara, S., Honke, K., Dickson, R.B., Lin, C.Y. and Taniguchi, N. (2002) Prometastatic effect of *N*-acetylglucosaminyltransferase V is due to modification and stabilization of active matriptase by adding beta 1–6 GlcNAc branching. J. Biol. Chem. 277, 16960–16967.

[7] Inamori, K., Endo, T., Ide, Y., Fujii, S., Gu, J., Honke, K. and Taniguchi, N. (2003) Molecular cloning and characterization of human GnT-IX, a novel {beta}1,6-*N*-acetylglucosaminyltransferase that is specifically expressed in the brain. J. Biol. Chem. 278, 43102–43109.

[8] Kaneko, M., Alvarez-Manilla, G., Kamar, M., Lee, I., Lee, J.K., Troupe, K., Zhang, W., Osawa, M. and Pierce, M. (2003) A novel beta(1,6)-*N*-acetylglucosaminyltransferase V (GnT-VB). FEBS Lett. 554, 515–519.

[9] Granovsky, M., Fode, C., Warren, C.E., Campbell, R.M., Marth, J.D., Pierce, M., Fregien, N. and Dennis, J.W. (1995) GlcNAc-transferase V and core 2 GlcNAc-transferase expression in the developing mouse embryo. Glycobiology 5, 797–806.

[10] Brodeur, G.M. (2003) Neuroblastoma: biological insights into a clinical enigma. Nat. Rev. Cancer 3, 203–216.

[11] Brodeur, G.M., Pritchard, J., Berthold, F., Carlsen, N.L., Castel, V., Castelberry, R.P., De Bernardi, B., Evans, A.E., Favrot, M. and Hedborg, F., et al. (1993) Revisions of the international criteria for neuroblastoma diagnosis, staging, and response to treatment. J. Clin. Oncol. 11, 1466–1477.

[12] Kato, C., Miyazaki, K., Nakagawa, A., Ohira, M., Nakamura, Y., Ozaki, T., Imai, T. and Nakagawara, A. (2004) Low expression of human tubulin tyrosine ligase and suppressed tubulin tyrosination/detyrosination cycle are associated with impaired neuronal differentiation in neuroblastomas with poor prognosis. Int. J. Cancer 112, 365–375.

[13] Taniguchi, N., Nishikawa, A., Fujii, S. and Gu, J.G. (1989) Glycosyltransferase assays using pyridylaminated acceptors: *N*-acetylglucosaminyltransferase III, IV, and V. Meth. Enzymol. 179, 397–408.

[14] Islam, A., Kageyama, H., Takada, N., Kawamoto, T., Takayasu, H., Isogai, E., Ohira, M., Hashizume, K., Kobayashi, H., Kaneko, Y. and Nakagawara, A. (2000) High expression of Survivin, mapped to 17q25, is significantly associated with poor prognostic factors and promotes cell survival in human neuroblastoma. Oncogene 19, 617–623.

[15] Takada, N., Isogai, E., Kawamoto, T., Nakanishi, H., Todo, S. and Nakagawara, A. (2001) Retinoic acid-induced apoptosis of the CHP134 neuroblastoma cell line is associated with nuclear accumulation of p53 and is rescued by the GDNF/Ret signal. Med. Pediatr. Oncol. 36, 122–126.

[16] Nicholson, D.W., Ali, A., Thornberry, N.A., Vaillancourt, J.P., Ding, C.K., Gallant, M., Gareau, Y., Griffin, P.R., Labelle, M. and Lazebnik, Y.A., et al. (1995) Identification and inhibition of the ICE/CED-3 protease necessary for mammalian apoptosis. Nature 376, 37–43.

[17] Tewari, M., Quan, L.T., O'Rourke, K., Desnoyers, S., Zeng, Z., Beidler, D.R., Poirier, G.G., Salvesen, G.S. and Dixit, V.M. (1995) Yama/CPP32 beta, a mammalian homolog of CED-3, is a CrmA-inhibitable protease that cleaves the death substrate poly(ADP-ribose) polymerase. Cell 81, 801–809.

[18] Guo, H.B., Lee, I., Kamar, M., Akiyama, S.K. and Pierce, M. (2002) Aberrant *N*-glycosylation of beta1 integrin causes reduced alpha5beta1 integrin clustering and stimulates cell migration. Cancer Res. 62, 6837–6845.

[19] Fernandes, B., Sagman, U., Auger, M., Demetrio, M. and Dennis, J.W. (1991) Beta 1–6 branched oligosaccharides as a marker of tumor progression in human breast and colon neoplasia. Cancer Res. 51, 718–723.

[20] Seelentag, W.K., Li, W.P., Schmitz, S.F., Metzger, U., Aeberhard, P., Heitz, P.U. and Roth, J. (1998) Prognostic value of beta1,6-branched oligosaccharides in human colorectal carcinoma. Cancer Res. 58, 5559–5564.

[21] Murata, K., Miyoshi, E., Kameyama, M., Ishikawa, O., Kabuto, T., Sasaki, Y., Hiratsuka, M., Ohigashi, H., Ishiguro, S., Ito, S., Honda, H., Takemura, F., Taniguchi, N. and Imaoka, S. (2000) Expression of *N*-acetylglucosaminyltransferase V in colorectal cancer correlates with metastasis and poor prognosis. Clin. Cancer Res. 6, 1772–1777.

[22] Dosaka-Akita, H., Miyoshi, E., Suzuki, O., Itoh, T., Katoh, H. and Taniguchi, N. (2004) Expression of *N*-acetylglucosaminyltransferase V is associated with prognosis and histology in non-small cell lung cancers. Clin. Cancer Res. 10, 1773–1779.
[23] Inamori, K., Mita, S., Gu, J., Mizuno-Horikawa, Y., Miyoshi, E., Dennis, J.W. and Taniguchi, N. (in press) Demonstration of the expression and the enzymatic activity of *N*-acetylglucosaminyltransferase IX in the mouse brain. Biochim Biophys Acta.
[24] Bown, N., Cotterill, S., Lastowska, M., O'Neill, S., Pearson, A.D., Plantaz, D., Meddeb, M., Danglot, G., Brinkschmidt, C., Christiansen, H., Laureys, G., Speleman, F., Nicholson, J., Bernheim, A., Betts, D.R., Vandesompele, J. and Van Roy, N. (1999) Gain of chromosome arm 17q and adverse outcome in patients with neuroblastoma. N. Engl. J. Med. 340, 1954–1961.
[25] Lastowska, M., Cotterill, S., Bown, N., Cullinane, C., Variend, S., Lunec, J., Strachan, T., Pearson, A.D. and Jackson, M.S. (2002) Breakpoint position on 17q identifies the most aggressive neuroblastoma tumors. Genes Chromosomes Cancer 34, 428–436.
[26] Yamamoto, H., Swoger, J., Greene, S., Saito, T., Hurh, J., Sweeley, C., Leestma, J., Mkrdichian, E., Cerullo, L., Nishikawa, A., Ihara, Y., Taniguchi, N. and Moskal, J.R. (2000) Beta1,6-*N*-acetylglucosamine-bearing *N*-glycans in human gliomas: implications for a role in regulating invasivity. Cancer Res. 60, 134–142.
[27] Guo, H.B., Lee, I., Bryan, B.T. and Pierce, M. (2005) Deletion of mouse embryo fibroblast *N*-acetylglucosaminyltransferase V stimulates alpha5beta1 integrin expression mediated by the protein kinase C signaling pathway. J. Biol. Chem. 280, 8332–8342.
[28] Dawson, G., Moskal, J.R. and Dawson, S.A. (2004) Transfection of 2,6 and 2,3-sialyltransferase genes and GlcNAc-transferase genes into human glioma cell line U-373 MG affects glycoconjugate expression and enhances cell death. J. Neurochem. 89, 1436–1444.

Oncogene (2006) 25, 5046–5055

www.nature.com/onc

ORIGINAL ARTICLE

Bcl-2 is a key regulator for the retinoic acid-induced apoptotic cell death in neuroblastoma

H Niizuma[1,2], Y Nakamura[1], T Ozaki[1], H Nakanishi[1], M Ohira[1], E Isogai[1], H Kageyama[1], M Imaizumi[3] and A Nakagawara[1]

[1]Division of Biochemistry, Chiba Cancer Center Research Institute, Chuoh-ku, Chiba, Japan; [2]Department of Pediatrics, Tohoku University School of Medicine, Aoba-ku, Sendai, Japan and [3]Department of Hematology and Oncology, Miyagi Children's Hospital, Aoba-ku, Sendai, Japan

Retinoic acid (RA) has been shown to induce neuronal differentiation and/or apoptosis, and is widely used as a chemotherapeutic agent for treating the patients with neuroblastoma. However, the therapeutic effect of RA is still limited. To unveil the molecular mechanism(s) inducing differentiation and apoptosis in neuroblastoma cells, we compared CHP134 and NB-39-nu cell lines, in which all-*trans*-RA (ATRA) induces apoptosis, with LA-N-5 and RTBM1 cell lines, in which it induces neuronal differentiation. Here, we found that Bcl-2 was strongly downregulated in CHP134 and NB-39-nu cells, whereas it was abundantly expressed in LA-N-5 and RTBM1 cells. ATRA-mediated apoptosis in CHP134 and NB-39-nu cells was associated with a significant activation of caspase-9 and caspase-3 as well as cytoplasmic release of cytochrome *c* from mitochondria in a p53-independent manner. Enforced expression of Bcl-2 significantly inhibited ATRA-mediated apoptosis in CHP134 cells. In addition, treatment of RTBM1 cells with a Bcl-2 inhibitor, HA14-1, enhanced apoptotic response induced by ATRA. Of note, two out of 10 sporadic neuroblastomas expressed *bcl-2* at undetectable levels and underwent cell death in response to ATRA in primary cultures. Thus, our present results suggest that overexpression of Bcl-2 is one of the key mechanisms to give neuroblastoma cells the resistance against ATRA-mediated apoptosis. This may provide a new therapeutic strategy against the ATRA-resistant and aggressive neuroblastomas by combining treatment with ATRA and a Bcl-2 inhibitor.
Oncogene (2006) **25,** 5046–5055. doi:10.1038/sj.onc.1209515; published online 27 March 2006

Keywords: apoptosis; Bcl-2; neuroblastoma; retinoic acid

Introduction

Neuroblastoma, which originates from the sympathoadrenal lineage of the neural crest, is one of the most common solid tumors in childhood and has distinct biological properties in different prognostic subsets (Schor, 1999). For example, tumors in patients less than 1 year of age often regress spontaneously and have a favorable prognosis. In contrast, tumors that occur over 1 year of age display an extensive and metastatic disease at diagnosis, and are often aggressive with an unfavorable prognosis despite an intensive therapy (Brodeur and Nakagawara, 1992). Each of those subsets shows various distinct genetic features including the ploidy status, *MYCN* amplification, allelic loss of the distal part of chromosome 1p and the gain of chromosome 17q (Brodeur, 2003). Additionally, high expression levels of neurotrophin receptors TrkA and TrkB are favorable and unfavorable prognostic indicators of neuroblastomas, respectively (Nakagawara *et al.*, 1993, 1994). Several lines of evidence suggest that the spontaneous regression of the favorable neuroblastomas is attributed at least in part to the developmentally programmed neuronal cell death and/or neuronal differentiation (Nakagawara, 1998). Indeed, the deprivation of nerve growth factor led to the massive cell death through apoptosis of neuroblastoma cells expressing TrkA (Nakagawara *et al.*, 1993).

Retinoic acids (RAs), which appear to be involved in vertebrate morphogenesis, are natural and synthetic derivatives of vitamin A (Maden, 2001; McCaffery *et al.*, 2003), and exert their biological functions through nuclear receptors including RA receptors (RARs) and retinoid X receptors (RXRs) (Lippman and Lotan, 2000). In response to RA binding, RAR/RXR heterodimers regulate the transcription of a number of target genes by binding to the specific DNA response elements (Balmer and Blomhoff, 2002). Retinoic acids have antitumor effects on neuroblastoma-derived cell lines accompanied by a marked decrease in the expression levels of *MYCN* (Thiele *et al.*, 1985). Studies utilizing cell lines also have revealed that neuroblastoma cell lines exposed to all-*trans*-RA (ATRA) undergo neuronal differentiation, cell cycle arrest and/or apoptosis (Melino *et al.*, 1997; van Noesel and Versteeg, 2004). Recent

Correspondence: Dr A Nakagawara, Division of Biochemistry, Chiba Cancer Center Research Institute, 666-2 Nitona, Chuoh-ku, Chiba 260-8717, Japan.
E-mail: akiranak@chiba-cc.jp
Received 8 November 2005; revised 6 February 2006; accepted 15 February 2006; published online 27 March 2006

works offer insights into the molecular mechanisms by which ATRA exerts its biological effects on neuroblastomas. All-*trans*-retinoic acid activates phosphatidylinositol 3′-kinase-Akt pathway that plays an important role in neuronal differentiation (Encinas *et al.*, 1999; Lopez-Carballo *et al.*, 2002), and it reduces the expression levels of MYCN (Thiele *et al.*, 1985) and upregulates the cyclin-dependent kinase (CDK) inhibitor $p27^{KIP1}$ in association with the ATRA-induced cell cycle arrest in neuroblastoma cells (Lee *et al.*, 1996; Nakamura *et al.*, 2003). In addition, certain neuroblastoma cells underwent apoptosis in response to ATRA (Piacentini *et al.*, 1992; Takada *et al.*, 2001; Nagai *et al.*, 2004). Consistent with these observations, 13-*cis*-RA treatment after intensive chemotherapy improved an event-free survival rate of the patients with aggressive neuroblastomas with 17% increase (Villablanca *et al.*, 1995; Matthay *et al.*, 1999). Although the antitumor effects of RA alone on aggressive neuroblastoma are limited, RA treatment has an advantage that it carries no severe side effects. Thus, it is important to enhance the antitumor effects of RA on neuroblastoma cells, and thereby inducing apoptosis.

In the present study, we have found that the ATRA treatment induces neuronal differentiation in neuroblastoma-derived LA-N-5 and RTBM1 cells, whereas CHP134 and NB-39-nu cells undergo p53-independent apoptotic cell death in response to ATRA. Extensive expression studies revealed that the antiapoptotic Bcl-2 was constitutively expressed at high levels in LA-N-5 and RTBM1 cells, whereas CHP134 and NB-39-nu cells expressed Bcl-2 at extremely low levels. Enforced expression of Bcl-2 in CHP134 cells led to a significant inhibition of the ATRA-mediated apoptosis. In accordance with these results, the treatment with Bcl-2 inhibitor in RTBM1 cells resulted in an increased sensitivity to ATRA. Moreover, two out of 10 sporadic neuroblastomas in primary cultures with undetectable *bcl-2* underwent cell death in response to ATRA, whereas seven tumors out of the remaining eight cases expressed high levels of *bcl-2*. These results suggest that Bcl-2 might be a key regulator for the ATRA-mediated apoptotic cell death in neuroblastomas.

Results

ATRA-induced growth inhibition, differentiation and cell death in human neuroblastoma cell lines

To examine the possible effects of ATRA on growth and viability of neuroblastoma cells, human neuroblastoma-derived LA-N-5, RTBM1, CHP134 and NB-39-nu cells were cultured with or without 5 μM of ATRA, and the numbers of viable cells were counted at the indicated time points after the exposure to ATRA. As shown in Figure 1a, ATRA effectively inhibited proliferation of these neuroblastoma cells. Among them, the growth of CHP134 and NB-39-nu cells was much more suppressed in the presence of ATRA. To monitor morphological changes induced by ATRA, ATRA-treated cells were checked by phase-contrast microscopy. As shown in Figure 1b, a neurite outgrowth was evident in ATRA-treated LA-N-5, RTBM1 and CHP134 cells, whereas it was marginal in NB-39-nu cells. Of note, ATRA-induced cell death was detectable in CHP134 and NB-39-nu cells, but not in LA-N-5 and RTBM1 cells. To confirm whether ATRA could induce the apoptotic cell death in CHP134 and NB-39-nu cells, we examined the changes in the number of cells with sub-G1 DNA content in response to ATRA. As shown in Figure 1c and d, the flow cytometric analysis revealed that the number of CHP134 cells with sub-G1 DNA content was significantly increased in response to ATRA. Similarly, ATRA promoted the apoptotic cell death in NB-39-nu cells, albeit to a lesser degree than CHP134 cells. Under our experimental conditions, ATRA failed to induce the apoptotic cell death in LA-N-5 and RTBM1 cells (data not shown).

ATRA-induced apoptotic cell death in neuroblastoma cells

To elucidate the molecular mechanism(s) underlying the ATRA-mediated apoptotic cell death in neuroblastoma cells, we examined whether the procaspases could be proteolytically cleaved to be activated in response to ATRA. To this end, whole-cell lysates prepared from the indicated neuroblastoma cells exposed to 5 μM of ATRA for 0, 2, 4 and 6 days were subjected to immunoblotting with the indicated antibodies. As shown in Figure 2a, the time-dependent proteolytic cleavage of caspase-9 and caspase-3 was observed in CHP134 and NB-39-nu cells, but not in LA-N-5 and RTBM1 cells. Consistent with these results, one of the physiological substrates of the activated caspase-3, poly-ADP-ribose polymerase (PARP), was cleaved in ATRA-treated CHP134 and NB-39-nu cells. In a good agreement with the previous observations showing that caspase-8 is epigenetically silenced in a high percentage of neuroblastoma cells (Teitz *et al.*, 2000; van Noesel *et al.*, 2003), caspase-8 was undetectable in LA-N-5, RTBM1 and CHP134 cells. In contrast, NB-39-nu cells expressed a large amount of procaspase-8. Procaspase-12, which is involved in the endoplasmic reticulum-stress-induced apoptosis (Nakagawa *et al.*, 2000; Morishima *et al.*, 2002), was readily detectable in all of the neuroblastoma cell lines that we examined, and did not respond to ATRA. Under our experimental conditions, ATRA had negligible effects on proteolytic cleavage of caspase-8 and caspase-12 (data not shown).

As caspase-9 is activated in response to the cytoplasmic release of cytochrome *c* from mitochondria, leading to the activation of caspase-3 (Degterev *et al.*, 2003), we sought to examine whether cytochrome *c* could be released in response to ATRA. To this end, CHP134 cells were treated with 5 μM of ATRA or left untreated, and cells were incubated with the antibody against cytochrome *c* or with the control immunoglobulin (Ig)G. Cell nuclei were stained with 4,6-diamidino-2-phenylindole (DAPI). Microscopic images demonstrated that cytochrome *c* staining displays a punctuate

cytoplasmic pattern in the absence of ATRA (Figure 2b, left). This staining pattern was almost identical to the MitoTracker staining (data not shown). ATRA treatment for 4 days induced redistribution of cytochrome *c* to a diffused cytoplasmic pattern in cells with apoptotic nuclei (Figure 2b, middle), suggesting

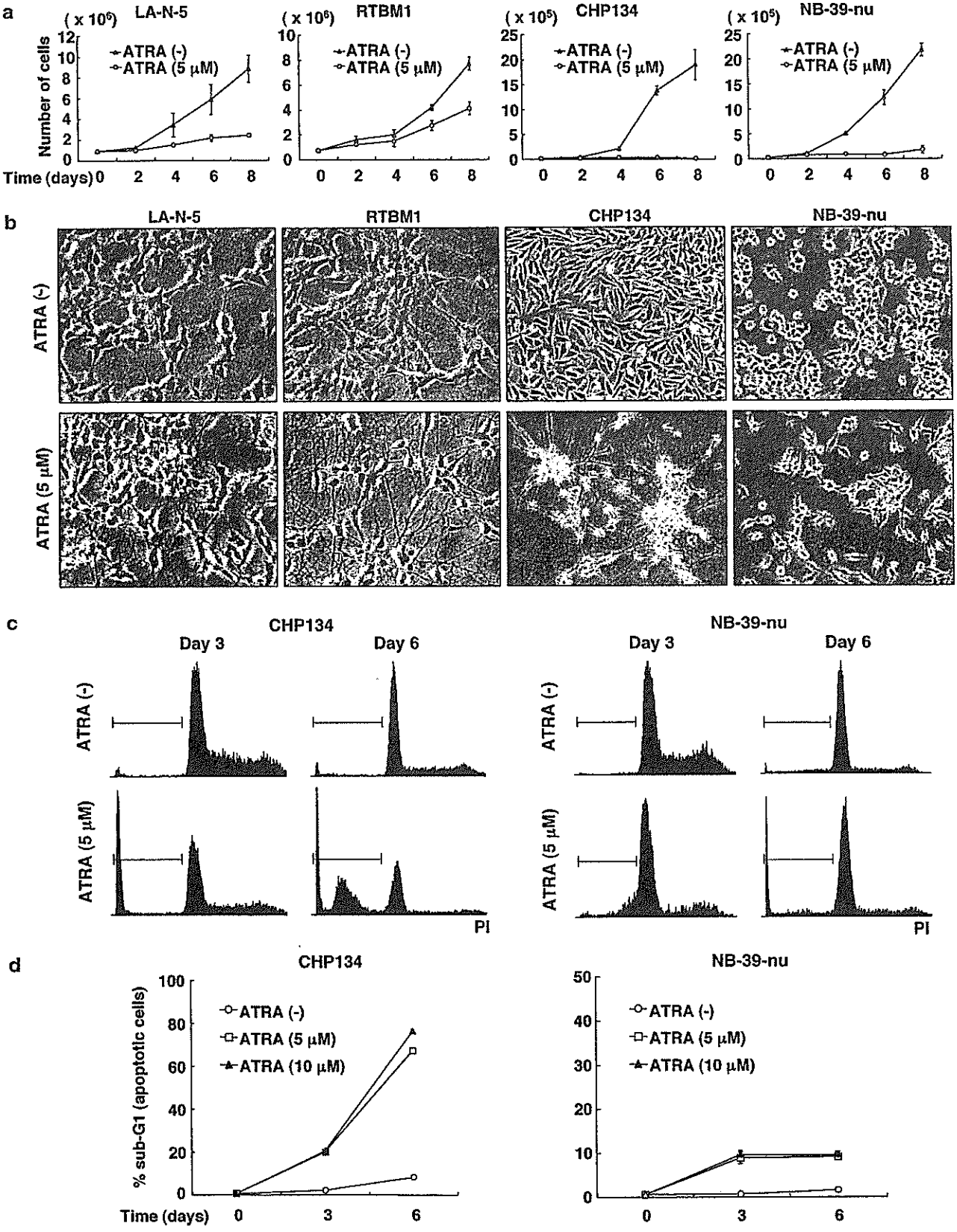

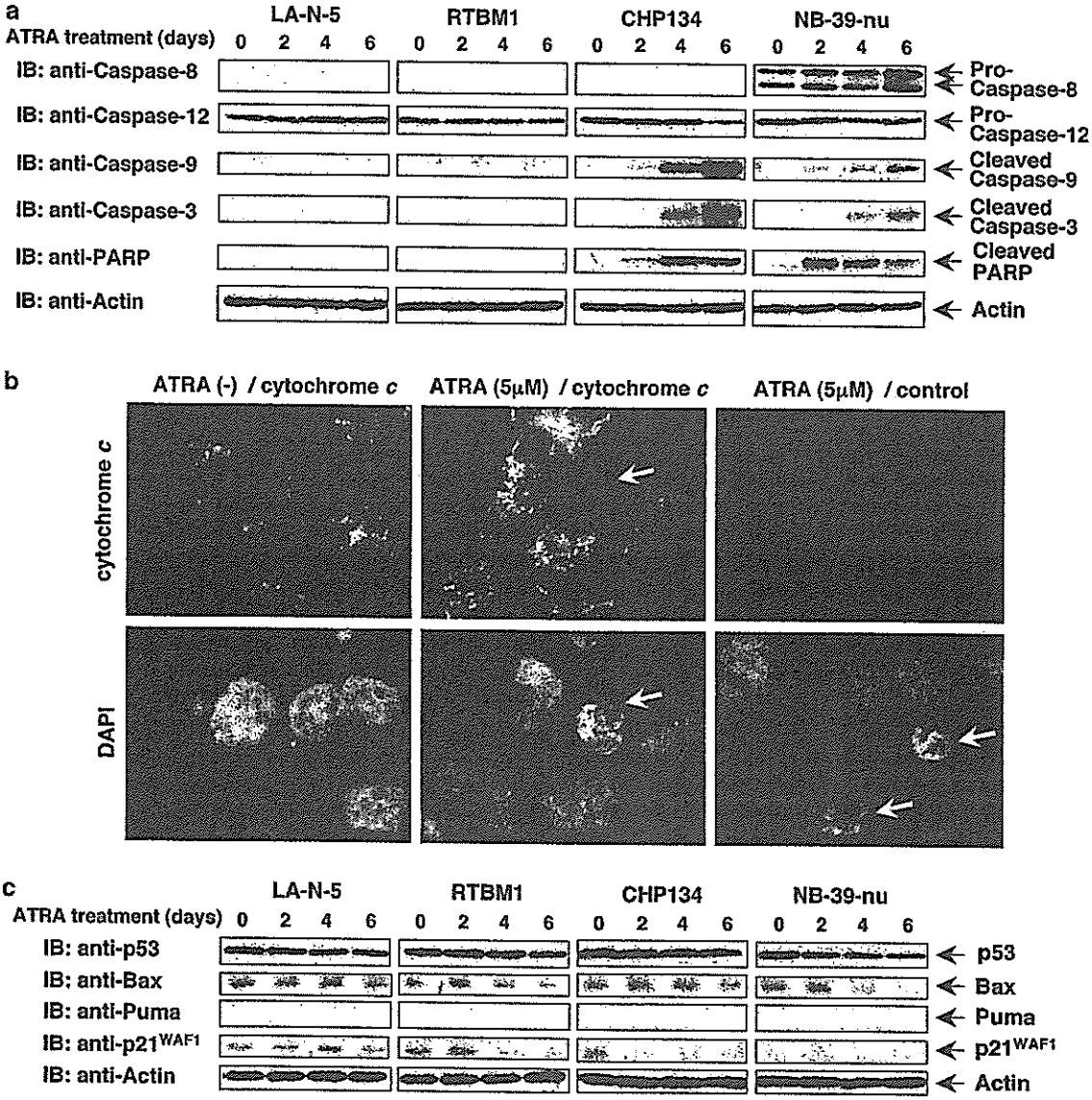

Figure 2 Caspase-9 and caspase-3 are cleaved during the all-*trans* retinoic acid (ATRA)-mediated apoptosis in CHP134 and NB-39-nu cells. (a) Immunoblot analysis for various caspases and poly-ADP-ribose polymerase (PARP) in response to ATRA. The indicated neuroblastoma cell lines were treated with 5 μM of ATRA or left untreated. At the indicated time points after the treatment with ATRA, whole-cell lysates were prepared, and analysed by immunoblotting with indicated antibodies. Actin expression was used as a loading control (bottom). (b) ATRA-induced cytoplasmic release of cytochrome *c* in CHP134 cells. CHP134 cells were seeded onto coverslips, and cultured in the presence or absence of 5 μM of ATRA. Four days after the treatment with ATRA, cells were fixed and stained with a monoclonal antibody against cytochrome *c* (top, left and middle) or with a normal mouse IgG (top, right). The cell nuclei were stained with 4,6-diamidino-2-phenylindole (DAPI) (bottom). The arrows indicate apoptotic cells with condensed and fragmented nuclei. (c) Expression levels of p53 and its direct target gene products in response to ATRA. At the indicated time periods after the treatment with ATRA, whole-cell lysates were prepared, and subjected to immunoblotting with antibodies against p53, Bax, Puma, $p21^{WAF1}$ and actin. Immunoblotting for actin is shown as a control for protein loading (bottom).

Figure 1 Effects of all-*trans* retinoic acid (ATRA) on cell proliferation of LA-N-5, RTBM1, CHP134 and NB-39-nu neuroblastoma-derived cell lines. (a) Growth curves of the indicated neuroblastoma cell lines in the presence or absence of ATRA. Cells were grown in the standard culture medium, and treated with 5 μM of ATRA. At the indicated time points after the treatment with ATRA, cells were trypsinized, harvested and number of viable cells was counted in triplicate. (b) ATRA-induced morphological changes of neuroblastoma cell lines. Cells were exposed to ATRA at a final concentration of 5 μM or left untreated. Six days after the treatment with ATRA, cells were examined by phase-contrast microscopy. (c and d) ATRA-induced cell death through apoptosis in CHP134 and NB-39-nu cells. Cells were treated with the indicated concentrations of ATRA or left untreated, and incubated for up to 6 days. At the indicated time points after the treatment with ATRA, cells were collected, fixed and stained with propidium iodide (PI). The DNA content of the cells was then examined by flow cytometry (c). The number of cells with sub-G1 DNA content was counted in triplicate (d).

that cytochrome *c* release from mitochondria might play an important role in ATRA-induced apoptotic cell death in neuroblastoma cells.

As the neuroblastoma cell lines that we examined carry wild-type p53 (data not shown), we investigated whether p53 could contribute to the ATRA-mediated apoptotic cell death. For this purpose, whole-cell lysates prepared from the indicated neuroblastoma cells exposed to 5 μM of ATRA for 0, 2, 4 and 6 days were processed for immunoblotting with the indicated antibodies. As shown in Figure 2c, the amounts of p53 remained unchanged or slightly decreased after ATRA treatment. In accordance with these results, ATRA had undetectable effects on the expression levels of p53-responsible Bax, Puma and $p21^{WAF1}$, which are implicated in the p53-dependent apoptosis and/or cell cycle arrest (Culmsee and Mattson, 2005). In addition, ATRA failed to induce the phosphorylation of p53 at Ser-15 (data not shown). Thus, it is likely that ATRA-mediated apoptotic cell death in neuroblastoma cells may be regulated in a p53-independent manner.

Differential expression of antiapoptotic Bcl-2 in neuroblastoma cells

To investigate the regulatory mechanisms of apoptotic response to ATRA in neuroblastoma cells, we examined the expression levels of Bcl-2 family proteins, which directly control the mitochondrial pathway of apoptosis. It is worth noting that antiapoptotic Bcl-2 was constitutively expressed at high levels in LA-N-5 as well as RTBM1 cells, whereas CHP134 and NB-39-nu cells expressed Bcl-2 at extremely low levels (Figure 3a). Antiapoptotic Bcl-x_L was expressed at low levels in all cell lines examined. In accordance with the previous observations showing that proapoptotic Bim and Bmf are highly expressed in neuronal cells (Puthalakath *et al*., 2001; Okuno *et al*., 2004; Shi *et al*., 2004), Bim and Bmf were expressed at high levels in all of the cell lines that we examined, but their expression levels remained unchanged in the presence of ATRA.

To determine whether Bcl-2 could contribute to the acquisition of the ATRA-resistant phenotype of neuroblastoma cells, CHP134 cells were transfected with the expression plasmid for Bcl-2 or with the empty plasmid, and their sensitivity to ATRA was examined by flow cytometry. As shown in Figure 3b, Bcl-2 was successfully overexpressed in CHP134 cells as examined by immunoblotting. Interestingly, enforced expression of Bcl-2 inhibited the ATRA-mediated proteolytic cleavage of caspase-3. Consistent with these results, flow cytometric analysis demonstrated that ectopic expression of Bcl-2 significantly reduced the number of cells with sub-G1 DNA content induced by ATRA treatment (Figure 3c and d), suggesting that Bcl-2 might play a critical role in the regulation of apoptotic cell death in neuroblastoma cells.

To further confirm this possibility, we examined the effects of the Bcl-2 inhibitor HA14-1 (Wang *et al*., 2000) on the ATRA-mediated apoptotic response of neuroblastoma cells. RTBM1 cells were treated with 5 μM of ATRA or left untreated for 6 days, and then incubated in the presence or absence of HA14-1 (15, 30 or 50 μM) for 3 h. Phase-contrast microscopic analysis showed that the incubation with ATRA followed by HA14-1 treatment significantly enhanced the apoptotic response of RTBM1 cells, whereas HA14-1 treatment alone increased the number of apoptotic cells to a lesser degree (Figure 4a). Similar results were also obtained by flow cytometric analysis (Figure 4b and c). To examine whether the ATRA-mediated apoptosis in RTBM1 cells induced by HA14-1 treatment could be associated with the activation of the mitochondria-dependent apoptotic pathway, we performed immunoblot analysis. As shown in Figure 4d, HA14-1 treatment at 30 μM or less did not promote the activation of caspase-9 and caspase-3, whereas a small amount of the cleaved caspase-9 and caspase-3 were detectable in RTBM1 cells exposed to 50 μM of HA14-1 alone. Intriguingly, pre-treatment of RTBM1 cells with ATRA enhanced the proteolytic cleavage of caspase-9 and caspase-3 induced by HA14-1 at a final concentration of 50 μM.

To ask whether Bcl-2 could play an important role in ATRA-mediated apoptotic response in primary neuroblastomas, 10 sporadically found neuroblastomas were subjected to both primary culture and reverse transcriptase–polymerase chain reaction (RT-PCR) analysis for *bcl-2*. In five cases, ATRA treatment induced strong outgrowth of neurites as compared with control culture (Figure 5a, left). In the other three cases, ATRA had undetectable effects (data not shown). It is worth noting that many cells underwent cell death after ATRA treatment in the remaining two cases (Figure 5a, right). We also examined the expression levels of *bcl-2* of these 10 primary neuroblastoma samples and four neuroblastoma-derived cell lines by RT–PCR. LA-N-5 and RTBM1 cells abundantly expressed *bcl-2*, whereas CHP134 and NB-39-nu did not (Figure 5b), which was consistent with immunoblotting as shown in Figure 3a. Of particular interest, RT–PCR analysis revealed that two primary cases that underwent cell death in response to ATRA (N-9 and N-10) expressed *bcl-2* at undetectable levels (Figure 5c). In a sharp contrast, the expression of *bcl-2* was detected in the remaining cases, except N-3. Taken together, our present results strongly suggest that Bcl-2 is a key regulator for ATRA-mediated apoptotic cell death in neuroblastoma cells.

Discussion

Retinoic acid is one of the potent antitumor agents that has been used successfully to treat certain human tumors including neuroblastomas (Freemantle *et al*., 2003). Indeed, neuroblastoma patients treated with RA have increased survival rate without severe side effects (Villablanca *et al*., 1995; Matthay *et al*., 1999). Accumulating evidences suggest that RA plays an important role in the regulation of neuroblastoma apoptosis as well as differentiation (Melino *et al*.,